


 Cite this: *Analyst*, 2025, **150**, 1206

# Recent advances in metallic and metal oxide nanoparticle-assisted molecular methods for the detection of *Escherichia coli*

 Linlin Zhuang,<sup>†a,b</sup> Jiansen Gong,<sup>†c</sup> Di Zhang,<sup>c</sup> Ping Zhang,<sup>c</sup> Ying Zhao,<sup>†b</sup> Li Sun,<sup>a</sup> Jianbo Yang,<sup>a</sup> Yu Zhang<sup>†\*b</sup> and Qiuping Shen<sup>†\*a</sup>

The detection of *E. coli* is of irreplaceable importance for the maintenance of public health and food safety. In the field of molecular detection, metal and metal oxide nanoparticles have demonstrated significant advantages due to their unique physicochemical properties, and their application in *E. coli* detection has become a cutting-edge focus of scientific research. This review systematically introduces the innovative applications of these nanoparticles in *E. coli* detection, including the use of magnetic nanoparticles for efficient enrichment of bacteria and precise purification of nucleic acids, as well as a variety of nanoparticle-assisted immunoassays such as enzyme-linked immunosorbent assays, lateral flow immunoassays, colorimetric methods, and fluorescence strategies. In addition, this paper addresses the application of nanoparticles used in nucleic acid tests, including amplification-free and amplification-based assays. Furthermore, the application of nanoparticles used in electrochemical and optical biosensors in *E. coli* detection is described, as well as other innovative assays. The advantages and challenges of the aforementioned technologies are subjected to rigorous analysis, and a prospective outlook on the future direction of development is presented. In conclusion, this review not only illustrates the practical utility and extensive potential of metal and metal oxide nanoparticles in *E. coli* detection, but also serves as a scientific and comprehensive reference for molecular diagnostics in food safety and public health.

 Received 1st December 2024,  
 Accepted 19th February 2025

DOI: 10.1039/d4an01495b

[rsc.li/analyst](https://rsc.li/analyst)

## 1 Introduction

### 1.1 Introduction to *E. coli*

*Escherichia coli* (*E. coli*) is a group of Gram-negative bacteria commonly found in the intestinal tracts of humans and animals, and some serotype strains are pathogenic under specific conditions and are classified as pathogenic *E. coli*, including enteropathogenic *E. coli* (EPEC), enterotoxigenic *E. coli* (ETEC), enteroinvasive *E. coli* (EIEC), enterohaemorrhagic *E. coli* (EHEC), enteroaggregative *E. coli* (EAEC), etc.<sup>1</sup> Of particular concern is the serotype O157:H7 of EHEC, which has the potential to cause enterohemorrhagic diarrhea and

severe urinary tract infections. Accurate detection of *E. coli* is crucial for public health safety and individual health, as they can exist as normal flora or cause food poisoning and other serious illnesses.

### 1.2 Overview of molecular methods for the detection of *E. coli*

At present, the most commonly utilized molecular techniques for *E. coli* detection are primarily immunoassays, nucleic acid-based tests (NATs), and biosensors. The immunoassays rely on the specific binding between antibodies and antigens. These include enzyme-linked immunosorbent assay (ELISA), immunofluorescence assays, lateral flow immunoassays (LFIs), etc.<sup>2</sup> ELISA is known for its high throughput, high sensitivity and good specificity. However, it is also time-consuming and cumbersome. Immunofluorescence methods are characterized by their high sensitivity and ease of use. However, they require costly equipment, and are susceptible to background interference. LFIs are rapid and convenient methods for point-of-care (POC) testing. It is important to note that these methods tend to exhibit reduced sensitivity. NATs are mainly used to detect specific genes of pathogenic bacteria, including polymerase chain reaction (PCR)-based technologies, isothermal

<sup>a</sup>School of Animal Husbandry and Veterinary Medicine, Jiangsu Vocational College of Agriculture and Forestry, Jurong 212400, P. R. China.

 E-mail: [qiupingshen@outlook.com](mailto:qiupingshen@outlook.com)
<sup>b</sup>State Key Laboratory of Digital Medical Engineering, Jiangsu Key Laboratory for Biomaterials and Devices, School of Biological Science and Medical Engineering & Basic Medicine Research and Innovation Center of Ministry of Education, Zhongda Hospital, Southeast University, Nanjing 211102, P. R. China.

 E-mail: [zhangyu@seu.edu.cn](mailto:zhangyu@seu.edu.cn)
<sup>c</sup>Poultry Institute, Chinese Academy of Agricultural Sciences, Yangzhou 225125, P. R. China

<sup>†</sup>These authors contributed equally to this work.

## Analyst

amplification assays, *etc.* PCR has the advantages of high sensitivity and specificity; however, it requires the use of sophisticated equipment and a complex operational procedure. Isothermal amplification is a rapid and straightforward method. However, experimental design and validation are intricate processes. Biosensors have high detection sensitivity, but are technically complex and costly. In light of the growing demand for rapid tests in low-resource settings, the World Health Organization (WHO) has outlined a set of ideal characteristics, known as the ASSURED criteria (affordable, sensitive, specific, user-friendly, rapid and robust, equipment-free, delivered to those who need it).<sup>3</sup> This has led to a relentless pursuit by researchers to develop ASSURED-type methods for *E. coli* detection.

### 1.3 Metal and metal oxide nanoparticles used in *E. coli* detection

With the development of nanoparticles (NPs) and nanotechnologies, the application of metal and oxide NPs in the field of microbial detection (*e.g.*, *E. coli*) has demonstrated significant advantages (Scheme 1).<sup>2</sup> These nanomaterials have become a significant driving force in the development of molecular detection technologies due to their distinctive physicochemical properties, such as high specific surface area, facile functional group modification, favorable biocompatibility, robust electrocatalytic activity, and extensive enzyme-like activity.<sup>4</sup> Specifically, the high specific surface area of the NPs has been demonstrated to enhance the sensitivity and speed of detection, thereby enabling the identification of target molecules



**Scheme 1** Metal and metal oxide nanoparticle-assisted methods for the detection of *E. coli*.

even in samples with low concentrations. Their rapid response capability fulfills the criteria for POC testing. The versatility afforded by the ease of modification enables these nanoparticles to serve a wide range of functions. The electrocatalytic activity of some nanoparticles has been shown to enhance the efficiency of electrochemical sensors. And the prevalence of enzyme-like properties in nanozymes renders them highly promising candidates for replacing natural enzymes.



**Yu Zhang's research group**

*Our research group is committed to the R&D, application, and industrialization of nanozymes, magnetic micro-/nanomaterials, molecular imaging, tumor diagnosis and treatment integration, biosensors, functional hydrogels, molecular/immunological diagnostic technologies, etc. Specifically, within the domain of molecular and immunological technologies for point-of-care testing (POCT), the research endeavors of our team center on the following areas: high-efficiency nucleic acid extraction, nucleic acid tests, high-performance fluorescent microspheres, and multi-cascade fluorescence signal amplification technologies. Additionally, we are engaged in the modification and application of functional micro-/nanomaterials, fluorescence immunochromatography, biosensors, etc. These research activities are directed towards providing theoretical and technical support for the expeditious and precise detection of foodborne pathogens, zoonotic pathogens, and disease-related molecular markers. Furthermore, the detection kits and equipment developed by the team are well suited for a variety of applications, including scientific research, medical diagnosis, food safety and quality testing, prevention and control of animal diseases, etc.*

## 2 Magnetic nanoparticle-based enrichment strategies

### 2.1 Capture of *E. coli* organisms

The application of magnetic nanoparticles (MNPs) in *E. coli* capture and enrichment has progressed significantly in research and has become one of the key technologies for the rapid and efficient detection of *E. coli* (Table 1). These nanoparticles are usually modified by surface modifications, such as polyethyleneimine (PEI), to enhance their binding ability to *E. coli*.<sup>5,6</sup> In addition, MNPs can be conjugated to other biomolecules such as antibodies, antimicrobial peptides, bacteriophages, or aptamers to improve capture specificity against *E. coli*.<sup>7–12</sup>

Additionally, it was determined that the surface charge of magnetic nanoparticles exerted a considerable influence on their capture efficiency. The positively charged magnetic nanoparticles (NP<sup>+</sup>) demonstrated a markedly enhanced capacity for bacterial capture in comparison with the negatively charged magnetic nanoparticles (NP<sup>-</sup>).<sup>6</sup> This charge-based capture mechanism is not dependent on a specific ligand, thereby conferring broader bacterial capture potential.

**Table 1** A summary of *E. coli* enrichment using MNPs

Nanoparticles	Modified groups	Target bacteria	Ref.
MNPs	Antibody	<i>E. coli</i>	13
MNPs	Phage receptor-binding protein (RBP)	<i>E. coli</i>	10
MNPs	Bacteriophages (T4, T7)	<i>E. coli</i> , <i>E. coli</i> K12	11, 14 and 15
MNPs	Concanavilin A (ConA)	<i>Staphylococcus aureus</i> , <i>E. coli</i> , and <i>Pseudomonas aeruginosa</i>	16
MNPs	PEI	<i>E. coli</i>	6
MNPs	Wulff-type boronic acid (B-N/APBA)	<i>E. coli</i> O157:H7	17
MNPs	Glycan	<i>E. coli</i> , <i>E. coli</i> O157, <i>Listeria monocytogenes</i> , and <i>Staphylococcus aureus</i>	18
MNPs	4-Formylphenylboric acid (FPBA)	<i>E. coli</i> O157, <i>Staphylococcus aureus</i>	19
MNPs	<i>N</i> -Trimethoxysilylpropyl- <i>N,N,N</i> -trimethylammonium chloride	<i>E. coli</i> , <i>Staphylococcus aureus</i>	20
MNPs	Mannose, D-mannose, galactose	<i>E. coli</i> , <i>E. coli</i> O157:H7	21 and 22
MNPs	$\beta$ -Lactam antibiotic amoxicillin	<i>E. coli</i> , <i>Staphylococcus aureus</i>	23
MNPs	Poly(ethylene glycol) (PEG), aptamers	<i>E. coli</i> , <i>Staphylococcus aureus</i>	24
MNPs	(3-Aminopropyl)triethoxysilane (APTES)	<i>E. coli</i> , <i>Staphylococcus aureus</i>	25
MNPs	Arginine-modified phosphorylated chitosan	<i>E. coli</i> , <i>Staphylococcus epidermidis</i>	26
MNPs	Amino groups	<i>E. coli</i>	27
MNPs	Polyclonal antibodies	<i>E. coli</i> O157:H7	28
MNPs	Diethylamine ethyl, polydiallyldimethylamine	<i>E. coli</i> , <i>Aeromonas</i> , <i>Salmonella</i> , <i>Pseudomonas</i> , <i>Enterococcus</i> , <i>Bacillus</i> , <i>Staphylococcus</i>	29
MNPs	Peptides	<i>E. coli</i> O157:H7, <i>Staphylococcus aureus</i> , and <i>Vibrio parahaemolyticus</i>	7
MNPs	Antimicrobial peptide (bacitracin)	<i>E. coli</i> , <i>Staphylococcus aureus</i> , and <i>Pseudomonas aeruginosa</i>	30
MNPs	Cationic ionic liquid	<i>E. coli</i> , <i>Pseudomonas aeruginosa</i> , and <i>Staphylococcus aureus</i>	31
Magnetic nanoparticle clusters	Antibodies	<i>E. coli</i>	32
Magnetic nanoclusters	Peptides	<i>E. coli</i>	12
Magnetic nanoparticle chains	PEI	<i>E. coli</i> O157	5
Fe <sub>3</sub> O <sub>4</sub> @Au	Antibodies	<i>E. coli</i>	8 and 33
Fe <sub>3</sub> O <sub>4</sub> @Au	Aptamer	<i>E. coli</i>	9
Fe <sub>3</sub> O <sub>4</sub> @Au	Wheat germ agglutinin	<i>E. coli</i> O157:H7	34
Fe <sub>3</sub> O <sub>4</sub> @Au	Cecropin 1	<i>E. coli</i> O157:H7, <i>Pseudomonas aeruginosa</i>	35
Fe <sub>3</sub> O <sub>4</sub> -Au	3-Mercaptophenylboronic acid (3-MBA), 1-decanethiol (1-DT)	<i>E. coli</i>	36
Fe <sub>3</sub> O <sub>4</sub> @Ag-MNPs	Vancomycin	<i>E. coli</i> , <i>Staphylococcus aureus</i>	37
Ag-MNP	ConA	<i>E. coli</i> , <i>Salmonella typhimurium</i> , and <i>Staphylococcus aureus</i>	38
Fe <sub>3</sub> O <sub>4</sub> @Al <sub>2</sub> O <sub>3</sub> NPs	Pigeon ovalbumin (POA)	<i>E. coli</i>	39
Cobalt ferrite nanoparticles	Amino	<i>E. coli</i> , <i>Staphylococcus aureus</i>	40
Magnetic zirconia nanoparticles	None	<i>E. coli</i> , <i>Staphylococcus aureus</i>	41
Platinum-coated magnetic nanoparticle clusters	Half-fragments of monoclonal antibodies	<i>E. coli</i>	42

In summary, a variety of strategies employing MNPs have exhibited remarkable efficacy in the enrichment of *E. coli*. Charge and anion-exchange-based strategies (e.g., PEI and diethylamine ethyl) offer the advantages of broad applicability and rapid response, making them suitable for preliminary screening and environmental microbiology research.<sup>5,6,29</sup> However, these strategies have low specificity and are susceptible to environmental influences (e.g., pH and ionic concentration).<sup>43</sup> Biomolecule-based strategies (e.g., antibodies and phages) are distinguished by their high specificity and multifunctionality, and they play a significant role in the development of biosensors.<sup>11,13–15</sup> However, stability and cost concerns limit their broader application. Nanocomposite strategies (e.g., Fe<sub>3</sub>O<sub>4</sub>@Au and Fe<sub>3</sub>O<sub>4</sub>@Al<sub>2</sub>O<sub>3</sub>) have enhanced detection sensitivity through multifunctional integration and

enhanced stability, facilitating subsequent experimental studies.<sup>35,37,39</sup> However, these strategies are complicated and costly to operate. Sugar and peptide-based strategies (e.g., mannose and glycan) have found application in biomedical research and biosensor development due to their favorable biocompatibility and environmental friendliness.<sup>18,21,22</sup> However, these strategies exhibit limited selectivity and stability. Consequently, in pragmatic applications, strategies must be judiciously selected or amalgamated according to particular requirements and experimental conditions to achieve efficient, specific, and economical capture and enrichment effects.

## 2.2 Nucleic acid extraction

Significant advancements have been made in the utilization of MNPs in the extraction of nucleic acids from *E. coli*, offering

**Table 2** A summary of nucleic acid extraction from *E. coli* using MNPs

Nanoparticles	Modified groups	Extracts	Bacteria	Ref.
MNPs	Carboxyl groups	Plasmid DNA	<i>E. coli</i>	49
MNPs	Amino groups	Plasmid DNA	<i>E. coli</i>	50
MNPs	Oligonucleotide probes	Genomic DNA	ETEC, <i>E. coli</i> O157, <i>Salmonella</i> spp., and <i>Listeria monocytogenes</i>	46 and 51
MNPs	Oligonucleotide probes	16S rRNA	<i>E. coli</i> O157:H7	52
Hedgehog-inspired MNPs	SiO <sub>2</sub>	DNA	<i>E. coli</i>	45
Magnetic silica beads	SiO <sub>2</sub>	Genomic DNA	<i>E. coli</i> O157:H7	53
Superparamagnetic nanoparticles	PEI	Plasmid DNA	<i>E. coli</i>	44

an efficient and rapid approach for molecular diagnostics (Table 2). These nanoparticles are typically composed of superparamagnetic materials (*e.g.*, Fe<sub>3</sub>O<sub>4</sub>), which can be augmented through surface functionalization techniques, such as the addition of SiO<sub>2</sub>, oligonucleotide probes, and PEI, to enhance their affinity for nucleic acids.<sup>44–46</sup> The use of MNPs in nucleic acid extraction allows for the rapid separation of the extracted material by magnetic force, thereby reducing the number of washing and centrifugation steps typically required in conventional methods. This simplifies the overall process and improves the efficiency of the extraction. Furthermore, the electrostatic interaction-based strategy allows for the rapid extraction and highly sensitive detection of nucleic acids.<sup>47</sup>

It was demonstrated that genomic DNA extracted from *E. coli* using MNPs exhibited high purity and concentration. Furthermore, the quality of DNA extracted can be enhanced by optimizing the quantity of MNPs and the concentration of PEG.<sup>48</sup> The superparamagnetic properties of MNPs enable the rapid aggregation and release of nucleic acids in the presence of an external magnetic field, thereby reducing the sample processing time and lowering the risk of cross-contamination.<sup>44</sup>

MNPs have been demonstrated to have a variety of applications in the extraction of *E. coli* nucleic acid. Strategies reliant upon charge interaction (*e.g.*, PEI) are well suited for rapid molecular diagnostics, food safety testing, and environmental monitoring due to their high adsorption efficiency and ease of operation.<sup>44</sup> However, these strategies are characterized by low specificity and susceptibility to environmental influences (*e.g.*, pH). Oligonucleotide probe modification strategies have been shown to be advantageous for biosensor development and specific pathogen detection due to their high specificity, versatility, and sensitivity.<sup>46,51,52</sup> However, probe design is complex, and stability needs to be improved. The strategy of surface modification groups (*e.g.*, amino and carboxyl groups) is widely used in biomedical research and food safety detection by enhancing binding ability, providing versatility and high purity extraction.<sup>49,50</sup> However, the functionalization process is complex and requires optimization of modification conditions. Consequently, in practical applications, the selection of appropriate strategies is contingent upon specific requirements. For instance, the charge interaction strategy is favored for expedited extraction, the oligonucleotide probe modification strategy is preferred for high specificity detection, and the strategy of surface modification groups is the prevailing choice in most cases.<sup>53</sup>

## 3 Immunoassays assisted by metal and metal oxide nanoparticles

### 3.1 ELISAs

ELISA is a technique that uses antigen–antibody specific binding and enzyme-catalyzed chromogenic substrates for the detection and quantification of specific molecules in biological samples. In recent years, researchers have developed a series of innovative metal and metal oxide nanoparticle-assisted ELISAs with the objective of improving the sensitivity and utility of *E. coli* detection. Among these, the ELISA developed using highly catalytic and stable Au@AuPt nanoparticles not only achieved a visual detection limit of 100 CFU mL<sup>-1</sup> but also eliminated the need for stringent low temperature for reagent storage.<sup>54</sup> Furthermore, the construction of a highly sensitive ELISA was achieved through the design of single-stranded DNA containing additional and anchoring blocks, combined with the quenching effect of fluorescent Ag nanoclusters.<sup>55</sup> Notably, ultrasensitive detection of *E. coli* O157:H7 was achieved by a novel ELISA based on DNA hybridization chain reaction (HCR) and biotin–streptavidin signal amplification.<sup>56</sup> Interestingly, a smartphone-based microfluidic fluorescence ELISA has been developed for the rapid quantification of *E. coli*, with a processing time of 25 minutes and detection performance comparable to that of high-performance automated immunoassays.<sup>57</sup>

Additionally, nanozymes with enzyme-like activity are of particular interest. The use of bimetallic PdRu nanozymes to supplant the natural enzyme not only markedly augmented catalytic activity, but also guaranteed high specificity and reproducibility.<sup>58</sup> Furthermore, the combination of gold and iron oxide nanozymes has enabled the development of an easily interchangeable sandwich ELISA platform, which has the potential to enhance detection efficiency.<sup>59</sup>

### 3.2 LFIAs

**3.2.1 Gold nanoparticle-assisted LFIAs.** LFIA is a rapid and straightforward on-site detection technique that employs the principle of antigen–antibody specific binding for qualitative or semi-quantitative detection through chromatography on test strips. In recent years, researchers have developed a series of novel LFIAs based on gold nanoparticles (AuNPs) and their composites with the objective of improving the sensitivity of *E. coli* detection. Among these methods, the polyallylamine

hydrochloride-mediated metal growth method has been shown to achieve highly controlled growth of copper shells on AuNPs, with a detection limit of 9.8 CFU mL<sup>-1</sup> for *E. coli* O157:H7.<sup>60</sup> Concurrently, the synthesis of gold superparticles *via* evaporation-induced self-assembly markedly enhanced the absorbance, thereby facilitating the expeditious and precise detection of *E. coli* O157:H7 in milk.<sup>61</sup> Furthermore, the implementation of innovative nanomaterials, including *p*-mercaptophenylboronic acid-modified AuNPs and plasmonic enhanced LFIA, has enhanced the sensitivity and practicality of *E. coli* detection.<sup>62,63</sup> It is noteworthy that a colorimetric/fluorescent dual-mode LFIA utilising dopamine-modified AuNPs has been demonstrated to achieve a sensitive detection of *E. coli* O157:H7 with a detection limit as low as 90.6 CFU mL<sup>-1</sup>.<sup>64</sup> Moreover, the utilization of bimetallic Ag–Au urchin-like hollow microspheres and bifunctional junction proteins has also led to a notable enhancement in the sensitivity of LFIA.<sup>65</sup> Notably, the incorporation of innovative nanolabels, including multifunctional gold shell-coated graphene oxide (GO) nanosheets, positively charged functionalized AuNPs, and gold nanorods, offers promising avenues for expedient and precise detection of *E. coli*.<sup>66–68</sup>

**3.2.2 MNP-assisted LFIAs.** An ultra-rapid visual method utilized *E. coli* O157:H7 protease to modify the optical response of a surface-modified MNP-specific peptide probe, achieving a detection limit as low as 12 CFU mL<sup>-1</sup>.<sup>69</sup> Another innovative approach used a portable LFIA combined with a personal glucose meter (PGM) as a reading tool to visualize and quantify *E. coli* O157:H7 using carboxyl-coated Fe<sub>3</sub>O<sub>4</sub> nanoparticles as a carrier for invertase and antibodies.<sup>70</sup> Additionally, a method utilising gold-plated magnetic nanoparticle clusters (Au@MNCs) and porous nitrocellulose strips has been developed, exhibiting high selectivity and sensitivity (10<sup>3</sup> CFU mL<sup>-1</sup>) in the detection of *E. coli* O157 in milk.<sup>71</sup> These methods not only enhance the sensitivity and specificity of the detection process but also facilitate practical applications and provide new technological tools in the field of food safety detection.

**3.2.3 Quantum dot-based LFIAs.** Researchers have developed a quantum dot (QD)-based LFIA that utilized immunomagnetic separation and nanoparticle dissolution-triggered signal amplification for the efficient visualization and quantitative detection of *E. coli* O157:H7.<sup>72</sup> *E. coli* O157:H7 was magnetically separated and labeled with silver nanoparticles (AgNPs), which were subsequently converted into silver ions to burst QD fluorescence for signal amplification. Moreover, another monoclonal antibody-based fluorescent LFIA has been shown to accurately detect *E. coli* O157:H7 in beef and river water through non-radiative energy transfer between GO and QDs, with a significantly reduced cost (60% lower than that of conventional LFIA).<sup>73</sup> And the results can be read using a portable reader or a smartphone.

**3.2.4 Platinum nanoparticle-assisted LFIAs.** Researchers have developed a variety of platinum nanoparticle (PtNP)-assisted LFIAs that have markedly enhanced the sensitivity of *E. coli* detection. One method employed the accumulation

of Pt–Au bimetallic nanoparticles in the test area to produce distinctive colored bands due to their high peroxidase activity, enabling visual and quantitative detection of *E. coli* O157:H7 with a sensitivity enhancement of over 1000-fold compared to traditional LFIA.<sup>74</sup> In another approach, a label-free and dual-readout LFIA was established using multifunctional nanocomposites combining magnetic-adhesion-color-nanozyme properties, providing a novel approach for the design of multifunctional probes. Detection limits of 10<sup>2</sup> and 10 CFU mL<sup>-1</sup> were achieved through colorimetric and catalytic quantitative analyses, respectively.<sup>75</sup> Furthermore, researchers synthesized a polydopamine-mediated magnetic bimetallic nanozyme (Fe<sub>3</sub>O<sub>4</sub>@PDA@Pd/Pt) with peroxidase-like activity as a probe in LFIA, which successfully detected *E. coli* O157:H7 in milk as low as 90 CFU mL<sup>-1</sup>.<sup>76</sup> These studies demonstrate the great potential of nanozymes in food safety detection.

**3.2.5 Other nanoparticle-assisted novel LFIAs.** To enhance the efficiency and precision of LFIAs, researchers have devised a range of innovative nanoparticle-assisted techniques. A multi-readout and label-free LFIA based on a nanozyme-bacteria-antibody sandwich pattern was developed for the rapid detection of *E. coli* O157:H7.<sup>77</sup> This method employed a functional nanozyme-mannose-modified Prussian blue as a recognizer and signal indicator, achieving a quantitative range of 10<sup>2</sup> to 10<sup>8</sup> CFU mL<sup>-1</sup>. Additionally, researchers investigated the potential of novel nanomaterials, including Cu<sub>2–x</sub>Se nanocrystals and silver enhancement strategies, to enhance the sensitivity of LFIA. In addition to functioning as “nanoantibodies” to recognize *E. coli* O157:H7, Cu<sub>2–x</sub>Se nanocrystals also exhibited peroxidase-like catalytic activity, thereby enhancing the efficiency of the detection process.<sup>78</sup> The silver enhancement strategy led to a notable reduction in the detection limit and an enhancement in detection sensitivity through a chemical reaction.<sup>79</sup> Specifically, the test strip was immersed in a microtube containing a mixture of silver nitrate and hydroquinone/citrate buffer (1 : 1). The catalytic reduction of silver ions on the surface of AuNPs resulted in a color change from red to black, thereby enhancing the signal produced by AuNPs.

Furthermore, in order to further enhance the performance of LFIAs, researchers have developed a variety of multifunctional nanocomposites. These include an Fe<sub>3</sub>O<sub>4</sub>@TCPP@Pd [TCPP, tetrakis(4-carboxyphenyl)porphyrin] nanocomposite enzyme with magnetic, colorimetric, and catalytic properties, as well as a zirconium based organic framework embedded in methylene blue.<sup>80,81</sup> These materials have not only enhanced the sensitivity and accuracy of the assay, but have also augmented the functionality and practicality of LFIAs.

Additionally, researchers have investigated the potential of using novel materials, including Au@Ag core-shell nanoparticles, lanthanide-complexed polymers, palladium–platinum (Pd–Pt) nanoparticles, and Eu(III)-doped polystyrene nanoparticles, as markers to enhance the sensitivity and specificity of LFIAs.<sup>82–85</sup>

### 3.3 Colorimetric immunoassays

**3.3.1 AuNP-based colorimetric strategies.** In recent years, researchers have developed a variety of innovative methods based on AuNPs and aptamers for the rapid and sensitive detection of pathogenic bacteria, including *Salmonella*, *Listeria monocytogenes*, and *E. coli*.<sup>86,87</sup> These methods not only simplify the detection process but also enhance the accuracy and specificity of detection. For instance, an assay employing AuNPs and an aptamer sensor demonstrated the capacity to detect multiple pathogenic bacteria concurrently with 96% accuracy and specificity in meat samples.<sup>88</sup> Another innovative biosensor, in conjunction with a smartphone imaging application, has demonstrated the capacity to achieve sensitive detection of *E. coli* O157:H7 with a detection limit as low as 50 CFU mL<sup>-1</sup> through the monitoring of color changes in AuNPs (Fig. 1).<sup>89</sup>

Additionally, researchers have investigated the potential of novel biorecognition elements, including phages, metastable aptamers, and cationic dyes in conjunction with AuNPs, to enhance the sensitivity and specificity of detection. For instance, a sensor based on phage M13 and AuNPs demonstrated the capacity to detect a diverse array of Gram-negative bacteria in less than an hour, exhibiting remarkable stability across different media.<sup>90</sup> Furthermore, a bridge DNA synthesis system assembled with an allosteric aptamer and AuNPs has the potential to significantly amplify bacterial signals and enable quantitative detection of low concentrations of pathogenic bacteria in water.<sup>91</sup> Other researchers have targeted bacterial 16S rRNA and employed cationic dyes (Victoria Pure Blue BO and methylene blue) to induce electrokinetic AuNP agglutination, thereby achieving highly sensitive detection of *E. coli*.<sup>92</sup>

To enhance the convenience and practicality of detection even further, researchers have also developed smartphone-based colorimetric aptamer sensors and microfluidic paper-

based analytical devices.<sup>93–95</sup> These devices offer the additional benefit of low cost and straightforward operation, while also facilitating rapid on-site detection of pathogenic bacteria. For example, a smartphone-based colorimetric aptasensor has effectively identified *E. coli* O157:H7 in milk by monitoring the color alteration of AuNPs with excellent reproducibility and specificity.<sup>94</sup> Besides, a microfluidic paper-based analyzer was capable of simultaneously monitoring Gram-negative bacteria and nitrite ions, thereby offering a highly effective instrument for water quality monitoring.<sup>93</sup> And an intelligent colorimetric sensing platform integrated with immunomagnetic separation has been developed for rapid detection of *E. coli* O157:H7 in food.<sup>96</sup> This platform demonstrates high analytical sensitivity (1.63 CFU mL<sup>-1</sup>), short detection time (3 hours), and excellent selectivity, which is expected to serve as a new on-site detection platform for foodborne pathogens.

**3.3.2 Nanozyme-based colorimetric strategies.** Nanozymes are defined as catalytically active nanomaterials that are capable of mimicking the catalytic reactions observed in natural enzymes.<sup>97</sup> Presently, researchers have investigated a multitude of pioneering nanozyme-based techniques for the colorimetric identification of *E. coli*. Among these, Au@MnO<sub>2</sub> nanoparticles were selected for the detection of *E. coli* due to their distinctive core-shell structure and exceptional catalytic capabilities.<sup>98</sup> The enzyme-induced color-coded single-particle counting method for monitoring the activity of  $\beta$ -galactosidase demonstrated a highly sensitive detection of *E. coli* with a detection limit down to 15 CFU mL<sup>-1</sup>, and was successfully applied to the monitoring of river water samples. Additionally, highly sensitive colorimetric detection methods utilising an enzyme-nanozyme cascade reaction and platinum-coated magnetic nanoparticle cluster (Pt/MNC) magnetophoretic chromatography have been developed.<sup>42,99</sup> These methods are capable of detecting *E. coli* at concentrations as low as 100 and 10 CFU mL<sup>-1</sup>, respectively.

In addition to the aforementioned methods, researchers have investigated the development of diverse strategies for colorimetric detection of bacteria utilising other nanomaterials, including dopamine-modified iron oxide nanoparticles, AuNPs with peroxidase-like activity, magnetic nanoparticles, and cobalt-based zeolitic imidazolate framework nanosheets (ZIF-67).<sup>100–103</sup> These methods facilitate rapid and sensitive detection of bacteria by catalyzing the color development reaction or inhibiting the catalytic activity of the nanomaterials. For instance, dopamine-modified Fe<sub>3</sub>O<sub>4</sub> nanoparticles have been demonstrated to inhibit their catalytic activity in the presence of bacteria, thereby enabling the detection of bacteria (Fig. 2).<sup>101</sup> Similarly, AuNPs with peroxidase-like activity have been shown to achieve label-free colorimetric detection of *E. coli* by catalyzing the color development reaction.<sup>102</sup> These methods are not only cost-effective and straightforward to implement but also provide novel approaches for the expeditious identification of bacterial pathogens.

**3.3.3 Other nanoparticle-assisted colorimetric strategies.** Researchers have developed a number of innovative colorimetric methods for the efficient detection of *E. coli*. Among



**Fig. 1** Schematic representation of the functionalized AuNP-assisted colorimetric strategy for the detection of *E. coli* O157:H7.<sup>89</sup>



**Fig. 2** Schematic representation of colorimetric *E. coli* detection by using nanozymes (e.g., dopamine-capped  $\text{Fe}_3\text{O}_4$  NPs and chitosan-coated  $\text{Fe}_3\text{O}_4$  NPs).<sup>101,103</sup>

these methods, a procedure based on *p*-benzoquinone-promoted formation of Au@Ag core-shell nanoparticles has been developed for the straightforward and sensitive detection of *E. coli* through a color change.<sup>104</sup> In a further approach, novel bacterial probes were synthesized using solvent-induced co-assembly and combined with a smartphone application to achieve highly sensitive colorimetric detection.<sup>105</sup> Moreover, another researcher constructed a colorimetric biosensor using copper selenide nanoparticles, which achieved a wide range of detection of *E. coli* O157:H7 through a sandwich structure (sample mixed with magnetic nanoprobe and nanozyme probes) and signal amplification (2,2'-azino-bis(3-ethylbenzothiazoline-6-sulfonate)–hydrogen peroxide reporting system).<sup>106</sup> Besides, a colorimetric method using nitroblue tetrazolium/5-bromo-4-chloro-3-indolyl phosphate, combined with immunomagnetic separation and selective filtration techniques, further enhanced the sensitivity of *E. coli* detection in lettuce samples.<sup>107</sup> Interestingly, researchers developed a technique based on silver nanorod array sensors, which enabled rapid differentiation between live and dead bacteria by monitoring the  $\text{H}_2\text{S}$  produced by the bacteria.<sup>108</sup> It is noteworthy that a smartphone-based detection platform can utilize aptamer-modified silica photonic microspheres for the quantification of *E. coli* O157:H7.<sup>109</sup> And this platform uses AuNPs and silver staining techniques to enhance analytical sensitivity ( $68 \text{ CFU mL}^{-1}$ ). These methods not only enhance the sensitivity and accuracy of detection but also streamline the operational process, offering robust support for *E. coli* detection in food safety and public health.

### 3.4 Fluorescence immunoassays

**3.4.1 AuNP-assisted fluorescence immunoassays.** Amino-functionalized AuNPs were employed as a model system to investigate the interaction between fluorescently labeled antibodies and AuNPs, with the objective of achieving rapid detection of *E. coli* O157:H7 in the range of  $10^3$  to  $10^5 \text{ CFU mL}^{-1}$ .<sup>110</sup> Furthermore, Au nanocluster-embedded chitosan nanocapsules were developed as a novel signal amplification system, which markedly enhanced the sensitivity of the assay ( $1 \text{ CFU}$

$\text{mL}^{-1}$ ). This approach was successfully employed for the detection of *E. coli* O157:H7 in drinking water and milk samples.<sup>111</sup> Another method, based on the immunomagnetic probe separation technique and the quenching effect of AuNPs on rhodamine B, enabled the sensitive detection of *E. coli* O157:H7 in milk with a detection limit of  $0.35 \text{ CFU mL}^{-1}$ .<sup>112</sup> Notably, a novel Förster resonance energy transfer (FRET) sensing platform was developed.<sup>113</sup> The interaction between gold nanoclusters and AuNPs enabled a one-step detection of *E. coli* O157:H7 with a detection limit as low as  $4 \text{ CFU mL}^{-1}$ , exhibiting high specificity and analytical sensitivity.

**3.4.2 QD-based fluorescence immunoassays.** Researchers have developed a variety of QD-based fluorescence immunoassays for the efficient detection of *E. coli*. These include methods using silane-functionalized glass substrates and antibody-conjugated cadmium telluride (CdTe) QDs, which demonstrated superior fluorescence properties and rapid detection of pathogenic bacteria.<sup>114</sup> In addition, other researchers have utilized MNPs in combination with a QD (CdTe and nickel-doped CdTe)-assisted microfluidic chip to achieve highly sensitive detection of *E. coli* and *Salmonella enteritidis*, with limits of detection as low as 5 and 3  $\text{CFU mL}^{-1}$ , respectively.<sup>115</sup> Another passive microfluidic chip based on sandwich immunoassay has also been developed for the rapid and sensitive detection of *E. coli* with a detection limit of  $5 \text{ CFU mL}^{-1}$ .<sup>116</sup>

In addition to the aforementioned methods, researchers investigated the potential of other fluorescent probes, including ZnSe/ZnS QDs and combinations of fluorescent carbon dots with AgNPs, for the detection of *E. coli*.<sup>117</sup> Among the probes tested, ZnSe/ZnS QDs demonstrated the most promising results, producing fluorescence microscopy images of bacteria and achieving a linear range of  $10^1$  to  $10^8 \text{ CFU mL}^{-1}$ . Furthermore, the combination of fluorescent carbon dots and AgNPs demonstrated effective detection of *E. coli* and *Staphylococcus aureus*, avoiding the fluorescence burst and exhibiting excellent bacterial killing efficiency.<sup>118</sup> Moreover, investigators have demonstrated the highly sensitive detection of *E. coli* using CdSe/CdS QDs and AuNP-assisted immunoassays.<sup>119,120</sup>

**3.4.3 Other nanoparticle-assisted fluorescence immunoassays.** Interestingly, researchers have developed a range of additional nanoparticle-based innovative fluorescence immunoassays for the efficient detection of *E. coli*. One notable example is a fluorescence immunoassay that employed a porous luminescent porous coordination network-224 (PCN-224) and AgNPs.<sup>121</sup> This approach demonstrated the capability to sensitively detect *E. coli* O157:H7 in milk, leveraging the fluorescence bursting effect of PCN-224 with a low detection limit of  $3.3 \times 10^2 \text{ CFU mL}^{-1}$ . The alternative approach employed antibiotic-functionalized cerium oxide ( $\text{CeO}_2$ ) nanoparticles and aptamer-modified AuNPs to achieve highly sensitive detection of *E. coli* through the mechanism of FRET.<sup>122</sup> The detection limit was as low as  $1.04 \text{ CFU mL}^{-1}$ , and the detection of *E. coli* in real samples could be accomplished within 30 minutes.

Furthermore, researchers have developed a highly sensitive immunoassay for the simultaneous detection of *E. coli* O157:H7 and *Salmonella typhimurium* using nanomaterials, including immunomagnetic nanobeads, MnO<sub>2</sub> nanoflowers, and QDs.<sup>123</sup> The method exhibited satisfactory recovery and analytical sensitivity in chicken samples. Concurrently, researchers developed an enhanced fluorescence analysis method based on the determination of *N*-acetyl- $\beta$ -D-glucosaminidase activity.<sup>124</sup> The addition of silica-coated zinc oxide (ZnO) nanoparticles enabled the sensitive detection of the severity of mastitis in dairy cows, facilitating the effective differentiation between healthy and diseased milk samples.

### 3.5 Other innovative nanoparticle-assisted immunoassays

Researchers have developed a number of innovative methods for the efficient detection of *E. coli* O157:H7 and other pathogenic bacteria. Among the methods developed, the one combining double-layer capillary-based high-gradient immunomagnetic separation, invertase-nanocluster-based signal amplification, and glucose meter-based signal detection achieved sensitive and rapid detection of *E. coli* O157:H7.<sup>125</sup> The low detection limit was found to be 79 CFU mL<sup>-1</sup>, indicating the potential for the method to detect other foodborne pathogens by modifying the antibodies. Moreover, ultra-sensitive on-site detection was achieved through the enumeration of *E. coli* under a dark-field microscope with the use of a magnetic nanoparticle probe.<sup>126</sup> With a detection sensitivity of 6 CFU  $\mu$ L<sup>-1</sup>, it is expected to be a versatile tool for on-site quantification of various pathogens.

In addition, research teams have investigated a range of technological tools, including an instant detection platform based on Au@Pt/SiO<sub>2</sub> NPs, and a POC immunoassay based on PtNP nanozymes and thermometer readings, with the aim of enhancing the sensitivity and speed of detecting *E. coli* O157:H7.<sup>127,128</sup> These methods demonstrated effective detection of *E. coli* O157:H7 by integrating immunomagnetic separation, colorimetric analysis, and signal amplification, with detection limits of 183 CFU mL<sup>-1</sup> and 14 CFU mL<sup>-1</sup>, respectively. Moreover, other researchers have employed magnetic Fe<sub>3</sub>O<sub>4</sub> organic-inorganic composites for immunomagnetic separation in conjunction with nanozyme PtNPs for signal amplification and thermometer readout for detection, thereby further enhancing the sensitivity and speed of the assay.<sup>128</sup>

Furthermore, researchers have developed a variety of technological tools for the detection of *E. coli* based on a multi-parametric magneto-fluorescent nanosensor,<sup>129</sup> Pt-nanoflower-assisted visual detection,<sup>130</sup> a polydopamine@copper ferrite-AgNP (PDA@CuFe<sub>2</sub>O<sub>4</sub>-AgNP)-assisted dual-signal readout detection platform,<sup>131</sup> the photothermal effect based on MPBA-AuNPs,<sup>132</sup> the CdSe QD attached magnetic bead-assisted microfluidic method,<sup>133</sup> and the AuNP-assisted barometer indicator.<sup>134</sup> These methods not only enhance the sensitivity and accuracy of detection but also streamline the operational process and reduce the cost of detection, thereby offering novel concepts and technical resources for the expeditious detection of pathogenic bacteria.

## 4 Metal and metal oxide nanoparticle-assisted NATs

### 4.1 Amplification-free strategies

**4.1.1 Colorimetric strategies.** AuNPs demonstrate considerable promise in the domain of biosensors, particularly in the identification of *E. coli* O157:H7. This is attributed to their distinctive colorimetric characteristics.<sup>135</sup> An AuNP-based biosensor that is capable of visually distinguishing between target and non-target DNA samples is shown in Fig. 3.<sup>136</sup> The biosensor exhibits high specificity and sensitivity to *E. coli* O157 DNA at a concentration as low as 2.5 ng  $\mu$ L<sup>-1</sup>, with detection occurring in less than 30 minutes. Moreover, a colorimetric biosensor based on random DNA double walkers and a colorimetric assay based on AuNPs and G-quadruplexes were also developed, with detection limits of 1 CFU mL<sup>-1</sup> and 1.35  $\times$  10<sup>2</sup> CFU mL<sup>-1</sup>.<sup>137,138</sup> These innovative colorimetric detection methods not only enhance the sensitivity and specificity of detection but also streamline the operational process, offering novel insights and technical resources for the expeditious identification of pathogenic bacteria.

**4.1.2 Fluorescence analysis strategies.** Researchers have developed a variety of innovative fluorescence analysis strategies for the efficient detection of *E. coli* and other microorganisms. Among these, fluorescent biosensors based on single-stranded DNA and carbon QDs-MNPs have demonstrated the capability to achieve highly sensitive detection of *E. coli* with a detection limit as low as 60 CFU mL<sup>-1</sup> through the monitoring of changes in fluorescence intensity.<sup>139,140</sup> Additionally, enzyme-mediated fluorescent biosensors developed through the use of a three-dimensional DNA walker and a catalytic hairpin assembly reaction strategy have exhibited the potential for rapid detection of *E. coli*.<sup>141</sup> Additionally, studies have been conducted to detect double-stranded DNA in live *E. coli* by a FRET method using RecA-green fluorescent protein.<sup>142</sup>

Additionally, researchers have investigated the potential of an AgNP-assisted filter paper-based fluorescent chemosensor and surface plasmon coupling electrochemiluminescence method for the detection of *E. coli*.<sup>143,144</sup> The combination of



Fig. 3 Schematic diagram of targeted aggregation of AuNPs for colorimetric detection of *E. coli* DNA.<sup>136</sup>

graphene QDs with oligonucleotide-modified AuNPs also demonstrated efficacy in the detection of *E. coli* O157:H7.<sup>145</sup>

Moreover, a novel 16S rRNA detection platform has been developed, which combined a sandwich hybridization reaction, single-molecule magnetic capture, and single particle-inductively coupled plasma mass spectrometry (ICP-MS) to achieve high-precision quantitative detection of the target with a detection limit of 10 fM.<sup>52</sup>

## 4.2 Nucleic acid amplification strategies

**4.2.1 Colorimetric strategies.** Researchers have developed numerous nanoparticle-assisted innovative colorimetric methods for efficient detection of *E. coli* amplicons. Among them, a dual-signal amplification strategy based on HCR of AuNPs and DNA-enhanced peroxidase-like activity achieved a highly sensitive visual detection of *E. coli* with a detection limit down to 28 CFU mL<sup>-1</sup>.<sup>146</sup> In addition, an aptamer targeting *E. coli* isolated using non-SELEX combined with a dual-signal amplification strategy further improved the sensitivity and specificity of detection.<sup>147</sup> Interestingly, an alternative approach employed magnetic beads that bind to biotin-labeled PCR products, which were then subjected to enzymatic deposition with silver and resulted in a discernible color change (Fig. 4).<sup>148</sup> Additionally, researchers have devised a novel approach for colorimetric detection of nucleic acids, employing cationic carbon dots to induce the aggregation and dispersion of AuNPs.<sup>149</sup>

Interestingly, researchers have investigated the potential of oligonucleotide-functionalized AuNPs for the direct detection of Shiga toxin-producing *E. coli* strains,<sup>150</sup> as well as multiplexed oligonucleotide ligation-PCR and general-purpose oligonucleotide microarrays incorporating AuNPs, for cost-effective and multiple detection of eight foodborne pathogens.<sup>151</sup>

**4.2.2 Fluorescence methods for analyzing products.** In order to enhance the performance of magnetic nanoparticle

polymerase chain reaction enzyme-linked gene assay, researchers have developed a solvent-sensitive nanoparticle-enhanced PCR assay for the detection of ETEC (Fig. 5a).<sup>152</sup> The novel assay not only enhances the detection limit but also markedly reduces the time required for the post-amplification process in comparison with conventional PCR. Furthermore, researchers have investigated the potential of a luminescence resonance energy transfer system based on upconversion nanoparticles (UCNPs), as well as a fluorescence burst-based sensing platform in conjunction with PCR for the rapid, sensitive, and specific detection of *E. coli* (Fig. 5b).<sup>153,154</sup> An alternative method employed a DNA composite-encapsulated DNA silver nanocluster/GO system for the determination of multiple



**Fig. 5** Schematic representation of two PCR-based assays for the detection of *E. coli*. (a) A solvent-sensitive nanoparticle-enhanced PCR assay for the detection of ETEC.<sup>152</sup> (b) A luminescence resonance energy transfer system based on UCNPs for the rapid detection of *E. coli*.<sup>154</sup>



**Fig. 4** Schematic representation of a magnetic bead-assisted hybridization assay.<sup>148</sup>

pathogens using rolling circle amplification (RCA).<sup>155</sup> It is noteworthy that researchers have achieved an ultra-rapid PCR assay that can differentiate multiple foodborne pathogens within 20 minutes by utilising the photothermal effect and high thermal conductivity of AuNPs.<sup>156</sup>

**4.2.3 LFIA-based strategies.** In recent years, a variety of isothermal amplification and LFIA-based methods have been developed for the rapid and sensitive detection of *E. coli*. Typically, the amplicon (primer or probe modifying a specific group) binds to a labeled antibody (e.g., AuNPs or fluorescence-labeled antibodies) in a binding pad. Subsequently, the complex binds to the specific antibody immobilized on the test line to form a detectable signal. The result is evaluated by the colorimetric or fluorescent signal of the test and control lines.<sup>157</sup>

One notable approach is the enzyme-free method, which employed isothermal strand displacement-HCR and LFIA to achieve visual and immediate detection of the 16S rRNA of *E. coli* O157:H7 with a detection limit as low as  $10^2$  CFU mL<sup>-1</sup>.<sup>158</sup> Another method combined aptamer-exonuclease III-assisted amplification and AuNP-LFIA for the detection of *E. coli* O157:H7, exhibiting a quantification capacity of 76 CFU mL<sup>-1</sup> within 4 hours.<sup>159</sup> Furthermore, a colloidal gold-based paper biosensor combined with LAMP and a smartphone enabled the visual detection of *E. coli* at 10–1000 CFU mL<sup>-1</sup> in spiked samples within 1 hour.<sup>160</sup>

Notably, PCR-based LFIA has been used for the multiplex detection of hygiene indicator bacteria, which can accurately detect *E. coli*, coliforms, and total bacteria with a limit of detection as low as 1 CFU mL<sup>-1</sup>.<sup>161</sup> Furthermore, EuNP-based biosensors coupled with recombinase polymerase amplification (RPA) can complete a single-tube amplification reaction in less than 15 minutes for the simultaneous quantitative detection of five foodborne pathogens (including *E. coli* O157:H7) with a sensitivity of 10 CFU mL<sup>-1</sup>.<sup>162</sup> Besides, the colorimetric LAMP-based LFIA was also used for the rapid and visual detection of *E. coli* O157:H7 with a detection limit down to 5.7 CFU mL<sup>-1</sup>.<sup>163</sup>

**4.2.4 Other novel analytical strategies.** An innovative platform utilising cyclic DNA nanostructure@AuNP tags and cascade primer exchange reaction achieved highly sensitive detection of *E. coli* O157:H7.<sup>34</sup> The platform was able to differentiate between target pathogens in complex samples and demonstrated accuracy comparable to quantitative PCR. In addition, the platform was able to detect low levels of *E. coli* O157:H7 in mouse serum. Another study developed a PGM-based label-free readout method for the PCR, which enabled rapid quantitative detection of DNA amplicons by exploiting the glucose oxidase-like activity of cerium oxide nanoparticles (CeO<sub>2</sub> NPs) (Fig. 6).<sup>164</sup> Meanwhile, a pressure sensor based on the gaseous generation reaction was also applied for *E. coli* detection.<sup>165</sup> Au–Pt alloy-coated AuNPs (Au@AuPtNPs) exhibited enhanced catalytic activity as innovative nanozymes capable of detecting *E. coli* O157:H7 at a concentration as low as 3 CFU mL<sup>-1</sup>. Furthermore, the simultaneous detection of *E. coli*, *Salmonella enterica*, and *Listeria monocytogenes* was



Fig. 6 Schematic diagram of a PGM-based readout of PCR products using the CeO<sub>2</sub> nanozyme.<sup>164</sup>

achieved through the use of silica MNP-assisted triplex PCR and electrochemical magneto genosensing, with detection limits ranging from 12 to 46 pg μL<sup>-1</sup>.<sup>166</sup> In addition, a detection system based on an asymmetric PCR and a microfabricated biochip was developed by analyzing the 16S ribosomal RNA gene, and successfully detected the five major pathogens that cause bovine mastitis.<sup>167</sup>

## 5 Metal and metal oxide nanoparticle-assisted biosensors

### 5.1 Electrochemical biosensors

**5.1.1 Impedimetric biosensors.** In recent years, a variety of impedimetric biosensors have been developed for the efficient detection of *E. coli* and its variants. Among them, an impedance-based DNA multiplex sensor capable of simultaneously detecting *E. coli* and its virulent f17 strains achieved highly sensitive detection of *yaiO* and *f17* genes using thiolated DNA dual probes and nanogold-modified electrodes.<sup>168</sup> Another impedimetric biosensor for the detection of *E. coli* using chemically synthesized bimetallic Ag–Au nanoparticles demonstrated a good linear range and low detection limit ( $10^1$ – $10^7$ , 18.8, cells per mL, respectively), and verified its usefulness in seawater and river water samples.<sup>169</sup> In addition, the affinity of mannose for *E. coli* hairs was utilized in conjunction with electrochemical impedance spectroscopy to develop a novel sensor for the rapid detection of *E. coli* with high selectivity and analytical sensitivity.<sup>170</sup>

In addition to the aforementioned methods, studies have explored the use of titanium dioxide (TiO<sub>2</sub>) nanoparticle-mediated impedimetric biosensor for the determination of *E. coli* O157:H7 DNA.<sup>171</sup> This method enables rapid detection through the measurement of current–voltage alterations. An additional impedimetric spectroscopy cellular sensor, based on the M13 phage, has been shown to exhibit high sensitivity and selectivity for the early detection of coliforms.<sup>172</sup>

Furthermore, researchers have developed a label-free impedimetric sensor using nickel nanoparticle-modified boron carbon nanorods as a platform to achieve rapid and sensitive detection of *E. coli* O157:H7.<sup>173</sup>

It is noteworthy that a novel method based on electrical impedance spectroscopy and MNPs coupled to a fork-finger electrode has been developed for the detection of a diverse range of pathogenic bacteria, including *E. coli*, *Staphylococcus aureus*, and *Salmonella typhimurium*, in both drinking water and apple juice.<sup>174</sup> The method does not necessitate sample preparation and is rapid for detection. Another highly sensitive detection platform, based on 3D cross-finger microelectrodes and bacterial metabolic activity, was demonstrated to be capable of detecting low concentrations of *E. coli* within one hour, thereby illustrating its potential for bacterial viability monitoring.<sup>175</sup> Interestingly, phage acts as a virus that specifically infects specific bacteria and selectively recognizes the target bacteria. This specific interaction between phage and bacteria exhibits remarkable thermal stability and resistance to environmental interference. A novel phage nanosensor achieved the sensitive detection of *E. coli* O157:H7 in food samples with high specificity and good recovery (90 to 108%).<sup>176</sup>

**5.1.2 Voltammetric biosensors.** In recent years, there have been notable advancements in the field of voltammetric biosensors, particularly in the rapid detection of *E. coli*. One electrochemical assay based on a dual-signal amplification strategy utilised screen-printed carbon electrodes modified with polyaniline (PANI) films and AuNPs for the detection of *E. coli* at a low concentration without DNA amplification.<sup>177</sup> Another method employed PANI-enclosed AuNPs as electrochemical markers in combination with antibody-specific recognition.<sup>178</sup> Moreover, there have been studies using aptamer-modified nanoparticle electrodes for the detection of *E. coli* O157:H7, as well as electrochemical methods based on bifunctional magnetic nanoparticle couplers, which have demonstrated favorable detection performance and specificity.<sup>179,180</sup>

Concurrently, electrochemical biosensors based on composite materials have also been extensively utilized for the detection of *E. coli*. For instance, a sensor created with the help of Prussian blue-multi-walled carbon nanotube–AuNP composites has demonstrated the capacity to rapidly and accurately detect *E. coli* through the use of a dynamic adjustment algorithm.<sup>181</sup> Furthermore, a portable sensor system enabled the rapid detection of *E. coli* and *Exiguobacterium aurantiacum* by means of an electrode pattern on a conductive glass substrate and a chitosan-stabilized AuNP sensing interface.<sup>182</sup> Besides, innovative electrochemical biosensors, including those composed of mesoporous ZrO<sub>2</sub>-Ag-G-SiO<sub>2</sub> and In<sub>2</sub>O<sub>3</sub>-G-SiO<sub>2</sub>, have demonstrated the ability to achieve highly selective and sensitive detection of *E. coli* O157:h7 using cyclic voltammetry.<sup>183</sup> The sensor also exhibited the capacity to recognize individual bacterial cells in a small sample volume.

**5.1.3 Other novel electrochemical biosensors.** In recent years, electrochemical methods have demonstrated significant advancements in the rapid detection of pathogenic bac-

teria, including *E. coli*. One such example is an electrochemical sandwich magnetic immunoassay constructed using Fe<sub>3</sub>O<sub>4</sub>@Au MNPs and screen-printed carbon electrodes.<sup>184</sup> Furthermore, research has been conducted to develop sandwich biosensors with electrochemical and fluorescence detection for the detection of F17-positive *E. coli* by synthesizing anti-F17A antibodies.<sup>185</sup> To enhance the sensitivity of detection, researchers have also investigated the integration of signal amplification techniques with nanoprobe, including MoS<sub>2</sub>-based nanoprobe, which have markedly enhanced the performance of electrochemical biosensors.<sup>186</sup> Additionally, a label-free capacitive immunosensor employed Au–Pt core-shell nanoparticles and graphene QDs to achieve highly sensitive recognition of trace *E. coli* in foodstuffs.<sup>187</sup> And electrochemical biosensing platforms based on 3D walker and enzyme-free toehold-mediated strand displacement, TiO<sub>2</sub> nanoparticles, and the CRISPR/Cas12a system exhibited high sensitivity and specificity.<sup>188–190</sup>

In addition to the aforementioned methods, photoelectrochemical (PEC) biosensors also demonstrate considerable potential for the detection of *E. coli*. For instance, a PEC aptasensor comprising bimetallic cerium/indium oxide nanocrystals with defects in mesoporous nitrogen-doped carbon has demonstrated high sensitivity towards the detection of *E. coli*. Similarly, high-performance PEC biosensing platforms based on non-metallic plasmonic tungsten oxide hydrate nanosheets (WO<sub>3</sub>·H<sub>2</sub>O) coupled with nitrogen-doped graphene QDs also achieved highly sensitive detection of *E. coli*.<sup>191,192</sup> Moreover, studies have been conducted on PEC sensors constructed using a mixture of triazine-based covalent-organic framework and Cu<sub>2</sub>O.<sup>193</sup> Additionally, a ratiometric electrochemical strategy based on capturing DNA-PANI/CuFe<sub>2</sub>O<sub>4</sub>/GO complexes has been developed, further broadening the application of PEC biosensors in *E. coli* detection.<sup>194</sup>

To enhance detection efficacy and diminish expenditure, researchers have additionally devised an array of innovative electrochemical biosensors. For instance, label-free electrochemical biosensors comprising AuNPs and boric acid moieties with strong affinity for diols, enabled the rapid differentiation between Gram-positive and Gram-negative bacteria.<sup>195</sup> Furthermore, the integration of graphene QDs and AgNPs with a smartphone as the excitation source and a device for capturing and processing the electrochemical signals facilitated real-time, highly sensitive (5 CFU mL<sup>-1</sup>) detection of *E. coli*.<sup>196</sup> Other studies have further enhanced the detection performance for *E. coli* by assembling flexible conductive paper electrodes and near-infrared (NIR)-responsive photoelectrochemical sensing platforms, as well as developing ultra-sensitive electrochemiluminescence/fluorescence dual-signal mode aptamer sensors and non-enzymatic sandwich-type electrochemical immunoassays.<sup>197–199</sup> Interestingly, the incorporation of organometallic nano-hybrids (e.g., AuNPs, CuNPs, etc.) and ZnO-CuO nanocomposites offers promising avenues for the concurrent detection of diverse pathogenic bacteria.<sup>200,201</sup>

## 5.2 Optical biosensors

**5.2.1 Fluorescence strategies.** Researchers have developed biosensors with multiple fluorescence strategies for the detection of *E. coli*. One approach combined superparamagnetic iron oxide nanoparticles and *E. coli*-specific aptamers to achieve qualitative and quantitative detection of *E. coli* using a magnetic separation technique. And a highly sensitive biosensor was constructed using CdTe QDs.<sup>202</sup> An alternative approach, based on the principle of FRET, has enabled the rapid, ultrasensitive, and specific detection of *E. coli* using a detection platform constructed with AuNPs and UCNPs.<sup>203</sup> In addition, scientists designed a guanidinium-functionalized UCNP-assisted fluorescent nanosensor that achieved simultaneous detection of seven common foodborne bacteria, including *E. coli*.<sup>204</sup> Moreover, a novel fiber-optic platform sensing scheme employed phage as a biorecognition element, thereby enabling rapid detection of *E. coli* on a fiber-optic platform.<sup>205</sup> And the scheme is specific for the host bacteria and can be employed for the detection of particular bacteria in mixed samples. Notably, tetraphenylethene-based covalent organic polymer nanoparticles exhibited robust fluorescence and electrochemiluminescence intensities, and the constructed biosensor demonstrated the capacity to detect *E. coli* with exceptional sensitivity ( $0.19 \text{ CFU mL}^{-1}$ ).<sup>206</sup>

**5.2.2 Surface-enhanced Raman scattering sensing strategies.** In recent years, researchers have developed a variety of surface-enhanced Raman scattering (SERS)-based biosensors and biosensing platforms for highly sensitive and selective detection of pathogenic bacteria such as *E. coli*. For instance, an integrated biosensor that incorporates magnetic enrichment and ratiometric SERS has demonstrated effective detection of *E. coli* and has been successfully employed in the analysis of a range of liquid foods.<sup>207</sup> Besides, studies have employed functionalized Au and AgNPs as SERS substrates, in conjunction with specific bacterial capture probes and SERS labels, to achieve quantitative detection of pathogenic bacteria, such as *E. coli*.<sup>208–211</sup> These sensing platforms demonstrate not only wide linear detection ranges and low detection limits but also good specificity and anti-interference capabilities.

To further enhance the sensitivity and convenience of detection, researchers have also investigated a range of innovative strategies. For example, one study synthesized SERS tags by integrating poly(4-cyanophene) nanoparticles and silver ions, which significantly amplify Raman signals under laser irradiation.<sup>212</sup> An alternative approach is the construction of SERS microarray chips utilising metal/semiconductor composites (ZnO@Ag) and ZnO nanoflowers. The chip is capable of not only monitoring the presence of pathogenic bacteria *in situ* but also inactivating them through the process of photocatalysis.<sup>213</sup> In addition, another study has employed a catalytic hairpin self-assembly-mediated cyclic signal amplification strategy to construct a ratiometric SERS aptasensor.<sup>214</sup> The sensor facilitates rapid and reliable detection of *E. coli* O157:H7 without the necessity of pre-culture or DNA extraction.

Additionally, researchers have developed a variety of SERS-based biosensing platforms for the rapid enrichment and ultrasensitive detection of bacteria.<sup>215</sup> These platforms typically integrate versatile SERS-active substrates with specific bacterial capture probes, thereby facilitating the efficient capture and identification of pathogenic bacteria.<sup>216–219</sup> Interestingly, the simultaneous collection of data from multiple chemical labels enabled these platforms to effectively differentiate between live and dead bacteria.

**5.2.3 Surface plasmon resonance sensing strategies.** In recent years, there have been notable advancements in the field of *E. coli* detection through the use of biosensors based on surface plasmon resonance (SPR) and localized surface plasmon resonance (LSPR). Researchers have developed a variety of SPR and LSPR biosensors for the efficient and sensitive detection of pathogenic bacteria such as *E. coli*. For example, a LSPR biosensor constructed using AgNPs demonstrated the capacity to detect *E. coli* with a detection limit as low as  $0.47 \text{ CFU mL}^{-1}$ .<sup>220</sup> Furthermore, surface-imprinted AuNPs have been employed as recognition elements, and the combination of the SPR technique achieved an ultra-sensitive detection of *E. coli* in urinary tract infections ( $1 \text{ CFU mL}^{-1}$ ).<sup>221</sup>

To enhance the efficacy and sensitivity of detection, researchers also investigated a range of innovative strategies. For instance, a magneto-plasmonic nanosensor that employed both SPR and spin–spin magnetic relaxation has demonstrated the capacity to rapidly and ultra-sensitively detect *E. coli* O157:H7 with a detection limit as low as 10 CFU.<sup>222</sup> Additionally, a fiber optic SPR sensor using AgNP-reduced GO (AgNP-rGO) nanocomposites as signal amplification elements demonstrated a notable enhancement in analytical sensitivity.<sup>223</sup>

In addition to the above techniques, researchers have developed a colorimetric biosensor utilising AuNPs in conjunction with responsive polymers.<sup>224</sup> The detection of *E. coli* and *Staphylococcus aureus* was achieved by monitoring changes in SPR. Besides, gold nanotwins have been employed for the selective photoelectronic detection of *E. coli* in human urine.<sup>225</sup>

## 5.3 Other innovative biosensors

A variety of innovative biosensors for the detection of *E. coli* have been developed by researchers. A complementary splitting resonator could achieve highly selective detection of *E. coli* and *Staphylococcus aureus* in aqueous media through the use of functionalized  $\text{Fe}_3\text{O}_4$ .<sup>225</sup> Another technique employed the use of NIR-induced fluorescent nanoparticles to construct sensitive and specific bacterial biosensors capable of simultaneously detecting and quantifying both Gram-positive and negative strains with a detection limit as low as  $20 \text{ CFU mL}^{-1}$ .<sup>226</sup> Furthermore, the use of AuNP-assisted amplification of microcantilever array biosensors enabled the rapid and accurate determination of a wide range of foodborne bacteria at ultra-low concentrations, including *E. coli* O157:H7 among others.<sup>227</sup>

In addition, researchers have developed a chemoresistive gas sensor and a “sense-and-treat” biosensor based on immu-

nomagnetic beads and metal–organic frameworks for the detection of *E. coli*.<sup>228,229</sup> The former employed a composite film comprising PANI and TiO<sub>2</sub> for the physical adsorption of gas molecules, whereas the latter combines the exceptional peroxidase activity of AgPt/PCN-223-Fe with highly efficacious antimicrobial properties under NIR light. Interestingly, researchers constructed a low-field nuclear magnetic resonance homogeneous sensor based on the click reaction triggered by *E. coli*, which enabled highly sensitive detection of *E. coli* through triple signal amplification.<sup>230</sup>

## 6 Other novel detection strategies

The advent of nanobiotechnology has witnessed the emergence of a plethora of ingenious techniques for the detection of pathogens. Among these, a number of methods have been devised that harness the distinctive attributes of nanoparticles to achieve the highly sensitive detection of bacteria. As an example, the inhibitory effects of ZnO nanoparticles and multi-walled carbon nanotubes on  $\beta$ -galactosidase activity enabled researchers to detect *E. coli* at a low concentration (10 CFU mL<sup>-1</sup>).<sup>231</sup> Moreover, researchers developed a novel approach for the rapid detection of *E. coli* using fluorescent probes of iron quantum clusters.<sup>232</sup> The method demonstrated effective recovery of Cu<sup>2+</sup>-induced fluorescence through the ability of *E. coli* to capture and reduce copper ions, thereby enabling rapid detection of *E. coli* within 30 minutes.

Moreover, researchers have investigated methodologies for the detection of bacteria with the use of nanomaterials, including QDs and AuNPs. For example, a multimodal detection method based on CdTe QDs has been shown to be highly sensitive for the detection of  $\beta$ -glucosidase and *E. coli*.<sup>233</sup> This has been achieved by a variety of means, including visualization, fluorescence, atomic fluorescence spectroscopy, and ICP-MS. Furthermore, researchers developed a method to indirectly detect bacterial concentration by detecting glucose concentration, which utilized the dual enzyme-like activity of AuNPs (glucose oxidase) and polyoxometalates (peroxidase) (Fig. 7).<sup>234</sup>

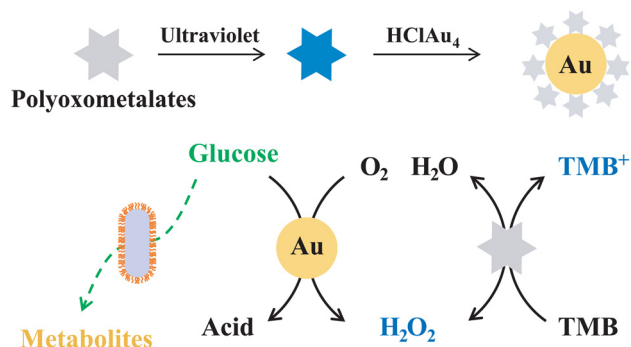


Fig. 7 Indirect detection of *E. coli* using dual enzyme-like activity detection of glucose concentration with AuNPs and polyoxometalates.<sup>234</sup>

To further enhance the simplicity and precision of detection, researchers have also devised innovative technologies, including acoustic bioprinters and photonic hydrogel platforms. The acoustic bioprinter facilitates the expeditious and precise identification of bacteria through the digitization of samples into millions of droplets, coupled with the use of SERS and machine learning algorithms.<sup>235</sup> Besides, the photonic hydrogel platform is capable of responding to pH alterations resulting from bacterial metabolism, thereby producing the corresponding color changes.<sup>236</sup> And the photothermal conversion ability could be employed to eradicate bacteria, thereby integrating visual diagnosis and on-site photothermal disinfection. Notably, an advancement in this field involves the integration of a colorimetric DNAzyme-crosslinked hydrogel sensor with an artificial intelligence (AI) model to achieve highly accurate pathogen detection, with 96% true positive and 100% true negative accuracy.<sup>237</sup> This development not only supports clinical applications but also holds significant potential to enhance population health outcomes.

Moreover, researchers have devised a multitude of novel approaches for the detection of *E. coli*. As an example, a fluorescence ON/OFF system that employs alkaline phosphatase expression in bacteria in conjunction with metal oxide nanoparticles facilitates the comprehensive detection of *E. coli*.<sup>238</sup> Additionally, an ICP-MS based method in conjunction with nanoparticle labeling was employed to concurrently detect a multitude of pathogenic bacteria in human blood samples.<sup>239</sup> Besides, studies have been conducted on the colorimetric strategy of AuNP aggregation triggered by the metabolic process of pathogenic bacteria, as well as a homogeneous fluorescent *E. coli* analytical system that employs  $\beta$ -galactosidase as a biomarker.<sup>240,241</sup> These studies have demonstrated high sensitivity and practicality.

## 7 Discussion and future prospects

### 7.1 MNPs used in *E. coli* enrichment and nucleic acid purification

The capture of *E. coli* can be achieved through the use of immunomagnetic nanoparticles that have been modified with specific moieties (*e.g.*, antibodies, aptamers, peptides, *etc.*) (Table 1). These nanoparticles combine the specificity of the immune response with the convenience of the magnetic response, allowing for the efficient capture of target bacteria through antigen–antibody interactions. Furthermore, the magnetic nanoparticles are capable of effectively capturing *E. coli* through electrostatic adsorption,<sup>6</sup> given that the surface of *E. coli* is negatively charged and that there is an electrostatic attraction between the positively charged magnetic nanoparticles (NP<sup>+</sup>) and the bacterial cells.

The utilization of MNPs in nucleic acid purification is predominantly predicated upon the tenets of solid-phase extraction. The surface modification of MNPs is of paramount importance for the efficiency of nucleic acid extraction. The most common modifications include the addition of amino

groups, carboxyl groups, hydroxyl, and oligonucleotide probes (Table 2). The functionalization of MNPs with amino groups led to a notable enhancement in the efficiency of DNA adsorption, with an increase of 4–5 times compared to unfunctionalized particles.<sup>242</sup> Amino- and carboxyl-modified magnetic beads adsorb nucleic acids using electrostatic adsorption and ionic bridges, respectively. Hydroxyl-modified magnetic beads enhance the adsorption capacity by forming hydrogen and chemical bonds with nucleic acids in a high-salt environment, thus extracting nucleic acids. Magnetic separation circumvents the laborious pipetting stage inherent to conventional methods, reducing operational time and the risk of contamination while facilitating increased automation.<sup>243</sup>

A plethora of MNP-based nucleic acid extraction kits have been commercialized for a diverse array of sample types. For example, a number of magnetic bead-based extraction kits have been employed in food safety monitoring, facilitating rapid and efficient extraction of nucleic acids from food samples.<sup>243</sup> Another study demonstrated the use of MNPs in the extraction of nucleic acids from *E. coli* O157:H7, showing that the quality of nucleic acids extracted by the instrument was comparable to that of commercial kits, but the extraction time was significantly shorter, being completed in only 50 minutes.<sup>244</sup>

It is important to note that the current nanoparticle-assisted *E. coli* enrichment and nucleic acid purification methods continue to encounter significant challenges in practical applications. From a cost and stability perspective, modified MNPs may be costly and require special preservation conditions, which limits their application in resource-limited environments.<sup>245</sup> The enrichment efficiency and specificity are influenced by factors such as bacterial concentration, pH, ionic strength, and bacterial surface structure. The enrichment efficiency and specific binding ability of low-concentration samples require further validation and enhancement. In the context of nucleic acid purification, although MNPs offer a reduction in operational steps, the process of dispersion and collection remains dependent on ancillary equipment (e.g., vortex mixer).<sup>246</sup> Additionally, the efficacy of impurity removal and the enhancement of purity and concentration require optimization, particularly in the context of complex sample processing. Furthermore, there is a necessity to enhance the portability and ease of operation of automated equipment to meet the demands of primary care and expedited testing in field settings.<sup>246</sup>

## 7.2 Metal and metal oxide nanoparticle-assisted immunoassays for *E. coli* detection

The use of metal and metal oxide nanoparticles in immunoassays has yielded novel strategies for the identification of *E. coli*. In ELISAs, nanoparticles (e.g., AuNPs, AgNPs, etc.) are utilized as signal amplifiers to augment the sensitivity and specificity of the detection.<sup>54,55</sup> AuNPs are frequently utilized to augment signal detection in ELISAs, largely due to their exemplary biocompatibility and facile surface modification capabilities. Additionally, nanozymes display enhanced stability,

adjustable activity, and multifunctionality compared to natural enzymes, making them a promising avenue for investigation in the context of ELISAs.<sup>58,59</sup>

The incorporation of nanoparticles (e.g., AuNPs, MNPs, PtNPs, etc.) into LFIA has also markedly enhanced the sensitivity and precision of detection.<sup>60,70,74</sup> Notably, QDs have been employed in the construction of non-radiative energy transfer-based detection platforms for the detection of *E. coli* due to their high stability and tunable emission wavelength.<sup>73</sup>

Interestingly, novel colorimetric immunoassays employ the optical characteristics of nanoparticles to facilitate the detection of *E. coli*. Colorimetric methods based on AuNPs are capable of detecting *E. coli* by monitoring changes in the dispersion and aggregation state of the nanoparticles.<sup>86,87</sup> Additionally, colorimetric methods based on nanozyme strategies employ the catalytic activity of nanoparticles (e.g., PtNPs, MNPs, etc.) to enhance the signal and achieve highly sensitive detection of the target.<sup>42,99,101</sup>

Moreover, certain metal and metal oxide nanoparticles are optimal materials for fluorescence signal enhancement, largely due to their distinctive optical characteristics. For example, AuNPs, AgNPs, MNPs, QDs, and other such materials have already demonstrated excellent potential for application in a variety of immunoassays.<sup>110,113–115</sup> The high specific surface area and excellent transport properties of nanomaterials allow for the loading of a large number of enzymes, antibodies, or other reactants on their surfaces, thereby achieving cascade signal amplification.

It is worth noting that the current nanoparticle-assisted immunoassays still face some challenges in *E. coli* detection. Complex sample matrices may undergo nanoparticle aggregation or non-specific adsorption, thereby affecting the efficacy of assays.<sup>247</sup> In addition, multi-target detection and quantitative analysis capabilities are still limited, and strategies such as the use of high-performance nanocomposite particles tend to increase the cost and operational complexity, and require trade-offs in space and time.<sup>248</sup> Meanwhile, some advanced signal amplification techniques require complex equipment support, limiting their application in resource-limited environments. Therefore, these technologies need to be further optimized in the future to improve sensitivity, specificity and stability. Concurrently, the operational complexity and cost are reduced to meet the actual detection needs.

## 7.3 Metal and metal oxide nanoparticle-assisted NATs for *E. coli* detection

The use of metal and metal oxide nanoparticle-assisted NATs has demonstrated considerable potential for the detection of *E. coli*. Amplification-free strategies, such as colorimetric and fluorescence analysis, facilitate rapid and intuitive detection of *E. coli* through the specific binding of nanoparticles to nucleic acids. In the colorimetric strategies, changes in the aggregation or dispersion state of the metal nanoparticles result in a color change, which is used to determine the presence of *E. coli* in the sample.<sup>135,136</sup> The fluorescence strategies quantify

the amount of *E. coli* present in a sample by measuring the enhancement or burst of fluorescence signal.<sup>139,140</sup>

The nucleic acid amplification strategies enhance the sensitivity and accuracy of the detection. Colorimetric detection of amplicons indirectly reflects the results of nucleic acid amplification by observing the color change of metal nanoparticles.<sup>148,149,151</sup> Fluorescence analysis of products employs the intensity of fluorescence signals to quantitatively evaluate the amplification efficiency.<sup>152–154</sup> Immunochromatographic strategies combine the specificity of antigen–antibody reactions with the signal amplification of metal nanoparticles, thereby achieving visual detection of *E. coli*.<sup>158,160,161</sup> Additional novel analytical strategies are being developed, including nanozyme-assisted product detection, electrochemical magneto genosensing, magnetoresistive sensors, *etc.*<sup>164–167</sup> These strategies aim to provide more diverse options for nucleic acid detection in *E. coli*.

Notably, amplification-free strategies (*e.g.*, colorimetric and fluorescence methods) often depend on alterations in the optical properties of nanoparticles to indicate the presence of target nucleic acids. However, these methods may lack the requisite sensitivity to detect low concentrations of *E. coli* in complex samples, such as food or environmental water samples. Besides, probes or antibodies modified on the surface of nanoparticles require high specificity to circumvent cross-reactivity with other components in the sample. However, non-specific binding may lead to false-positive results. Additionally, when combining nucleic acid amplification techniques with nanoparticles, it is essential to meticulously optimize the reaction conditions to mitigate cross-contamination and enhance detection efficiency.<sup>249</sup> Furthermore, certain detection techniques, particularly those reliant on colorimetric or fluorescence methods, necessitate the optimization of operational procedures to enhance their feasibility and economic viability in practical detection.

#### 7.4 Metal and metal oxide nanoparticle-assisted biosensors for *E. coli* detection

In recent years, electrochemical and optical sensors assisted by metals or metal nanoparticles have demonstrated significant potential for applications in the detection of *E. coli*. In the context of electrochemical sensors, impedimetric biosensors have demonstrated the capacity to achieve highly sensitive detection of *E. coli* through the monitoring of impedance changes resulting from bacterial adsorption.<sup>169–171</sup> Voltammetric biosensors, on the other hand, employ the redox reaction between the bacteria and the electrode surface to generate current signals, thereby enabling the rapid quantitative analysis of *E. coli*.<sup>179,180</sup> Furthermore, significant advancements have been made in the field of optical sensors. These include the development of fluorescence sensors, which generate fluorescence signals in the presence of specific probes (*e.g.*, CdTe QDs, AuNPs, UCNPs, *etc.*) interacting with *E. coli*, and SERS sensors.<sup>202,203,208–211</sup>

In addition to the above sensors, other novel biosensors have also played a significant role in the detection of *E. coli*. A

complementary split-ring resonator utilized the alteration in resonance frequency resulting from mass variation to identify *E. coli*, offering the benefits of high sensitivity.<sup>25</sup> And NIR-based biosensors facilitated rapid and non-destructive detection through the observation of spectral alterations induced by bacterial activity.<sup>226</sup> A microcantilever array biosensor integrated microfluidic and biometric components to facilitate high-throughput detection of *E. coli*.<sup>227</sup> Notably, chemoresistive gas sensors indirectly detected the presence of *E. coli* by monitoring the gas changes produced by bacterial metabolism.<sup>228</sup> The advent of these innovative sensors has established a novel technological platform for the expeditious and precise detection of *E. coli*, thereby enhancing the efficiency and efficacy of food safety monitoring.

Notably, electrochemical sensors are susceptible to electrode material degradation, signal drift, and interference from complex samples, although they are characterized by high sensitivity and fast response.<sup>250</sup> Optical sensors based on fluorescence strategies are susceptible to interference from other fluorescent substances, which can lead to an elevated background signal.<sup>251</sup> SERS and SPR offer high sensitivity in detection, but they face challenges in maintaining signal stability and reproducibility, particularly when dealing with complex samples. Furthermore, these sensors typically necessitate sophisticated equipment support (*e.g.*, electrochemical workstations, lasers, spectrometers, *etc.*) and specialized operators, limiting their application in resource-limited environments.

#### 7.5 Innovative application of nanozymes in the detection of *E. coli*

Nanozymes, as nanomaterials with natural enzyme catalytic activity, demonstrate considerable potential for use in the detection of *E. coli* due to their high stability, ease of storage, and ability to maintain activity under strict physiological conditions (Table 3). Metals and metal oxide nanoparticles are highly efficient in catalyzing substrates for colorimetric detection. The use of nanozymes in immunochromatographic methods serves to enhance the sensitivity and specificity of detection. Magnetic nanozymes can be utilized to isolate and enrich target bacteria under a magnetic field, subsequently facilitating catalytic reactions for the purpose of detection. Moreover, polymetallic nanozymes enhance both the efficiency of catalytic reactions and detection. In the future, it is anticipated that the rapid and accurate detection of *E. coli* and other pathogenic bacteria will be facilitated, thereby enhancing public safety and human health.

At present, nanozyme-based assays show great potential for *E. coli* detection applications but also face some challenges. The specificity of nanozymes is largely dependent on their surface modifications and catalytic mechanism, but in complex samples, non-specific binding may lead to false-positive results.<sup>256</sup> And the catalytic activity of nanozymes may be inhibited by other components in the sample. In addition, despite the ability of nanozymes to amplify signals through catalytic reactions, the analytical sensitivity may still be insufficient for detecting low concentrations of *E. coli* in complex

Table 3 Nanozymes used in the molecular methods for the detection of *E. coli*

Nanoparticles	Nanozymes	Catalytic activities	Substrates	Analytical strategies	Targets	Detection limit (CFU mL <sup>-1</sup> )	Detection/linear range (CFU mL <sup>-1</sup> )	Ref.
Au	AuNPs	Peroxidase	TMB	Colorimetric method	<i>E. coli</i>	28	2.5 × 10 <sup>2</sup> to 1.25 × 10 <sup>7</sup>	146
Au	AuNPs	Peroxidase	TMB	Colorimetric method	<i>E. coli</i>	15	1 × 10 <sup>2</sup> to 1 × 10 <sup>9</sup>	99
Au	AuNPs	Peroxidase	TMB	Colorimetric method	<i>E. coli</i>	5 × 10 <sup>3</sup> (visual), 75 (UV-vis spectrum)	5 × 10 <sup>2</sup> to 1 × 10 <sup>6</sup>	102
Au	AuNP@polyoxometalate	Glucose oxidase	Glucose	Visible spectrum	<i>S. aureus</i> and <i>E. coli</i>	5	1 to 7.5 × 10 <sup>7</sup>	234
Au	AuNPs	Peroxidase	H <sub>2</sub> O <sub>2</sub>	Immunosensor	<i>E. coli</i>	80	10 <sup>2</sup> to 10 <sup>7</sup>	134
Pt	PNPs	Peroxidase	H <sub>2</sub> O <sub>2</sub>	Thermometer reading	<i>E. coli</i> O157: H7	14	10 to 10 <sup>7</sup>	128
Pt	Zr-MOF modified with Pt-PCN-224 <sup>a</sup>	Peroxidase	TMB	Microfluidic biosensor	<i>E. coli</i> O157: H7	2	2.93 × 10 <sup>2</sup> to 2.93 × 10 <sup>8</sup>	252
Pt	PPNs <sup>b</sup>	Peroxidase	Ammonia-borane complex	Hydrogen detector	<i>E. coli</i> O157: H7	10	10 to 10 <sup>4</sup>	253
Fe	Fe <sub>3</sub> O <sub>4</sub>	Peroxidase	ABTS <sup>c</sup>	Colorimetric method	<i>E. coli</i> and <i>S. aureus</i>	10 <sup>4</sup> (visual), 10 <sup>2</sup> (spectrophotometry)	10 <sup>2</sup> to 10 <sup>6</sup>	103
Co	Cobalt-based ZIF-67 <sup>d</sup>	Peroxidase	TMB	Colorimetric method	<i>E. coli</i> O157: H7	12	3 × 10 <sup>1</sup> to 3 × 10 <sup>8</sup>	100
CeO <sub>2</sub>	CeO <sub>2</sub> NPs	Glucose oxidase	Glucose	PGM	<i>E. coli</i>	10 copies	10 to 10 <sup>4</sup> copies	164
Au, Pt	Au@PtNPs	Peroxidase	H <sub>2</sub> O <sub>2</sub>	Gas pressure sensor	<i>E. coli</i> O157: H7	5.3 × 10 <sup>2</sup>	1.6 × 10 <sup>3</sup> to 1.6 × 10 <sup>7</sup>	254
Au, Pt	Au@AuPt NPs	Peroxidase	TMB	ELISA	<i>E. coli</i> O157: H7	100 (visual), 59 (spectrophotometer)	10 <sup>2</sup> to 10 <sup>7</sup> (spectrophotometer)	54
Au, Pt	Au-Pt NPs	Peroxidase	TMB	Colorimetric method	<i>E. coli</i> O157: H7	2	10 to 10 <sup>7</sup>	255
Au, Pt	Au@Pt	Peroxidase	H <sub>2</sub> O <sub>2</sub>	Electrochemical immunoassay	<i>E. coli</i> O157: H7	4.5 × 10 <sup>2</sup>	4 × 10 <sup>3</sup> to 4 × 10 <sup>8</sup>	197
Au, Fe	Fe <sub>3</sub> O <sub>4</sub> and Au NPs	Peroxidase	TMB	LFIA	<i>E. coli</i> O157: H7	~10 <sup>3</sup>	10 <sup>3</sup> to 10 <sup>7</sup>	59
Pt, Au	Pt-Au NPs	Peroxidase	TMB	LFIA	<i>E. coli</i> O157: H7	10 <sup>2</sup> cells per mL	10 <sup>2</sup> to 10 <sup>8</sup> cells per mL	74
Pd, Pt	Fe <sub>3</sub> O <sub>4</sub> @PDA@Pd/Pt	Peroxidase	DAB <sup>e</sup>	LFIA	<i>E. coli</i> O157: H7	90	10 <sup>2</sup> to 10 <sup>5</sup>	76
Pd, Pt	Pd-Pt	Peroxidase	TMB	LFIA	<i>E. coli</i> O157: H7	87 (PBS <sup>f</sup> ), 900 (milk)	10 <sup>2</sup> to 10 <sup>6</sup> (PBS), 10 <sup>3</sup> to 10 <sup>6</sup> (milk)	85
Pd, Ru	PdRu	Peroxidase	TMB	ELISA	<i>E. coli</i> O157: H7	8.7 × 10 <sup>2</sup>	1.1 × 10 <sup>5</sup> to 2.8 × 10 <sup>7</sup>	58
Fe <sub>3</sub> O <sub>4</sub> , Pd	Fe <sub>3</sub> O <sub>4</sub> @TCPP@Pd	Peroxidase	TMB	LFIA	<i>E. coli</i> O157: H7	77	7 to 8 × 10 <sup>6</sup>	81
Ag, Pt, Fe	AgPt/PCN-223-Fe	Peroxidase	TMB	Colorimetric biosensor	<i>E. coli</i> O157: H7	276	10 <sup>3</sup> to 10 <sup>8</sup>	229

<sup>a</sup> MOF indicates metal-organic framework. <sup>b</sup> PPNS indicate peptide-Cu<sub>3</sub>(PO<sub>4</sub>)<sub>2</sub> hybrid nanocomposites with embedded PtNPs. <sup>c</sup> ABTS indicates 2,2'-azino-bis(3-ethylbenzothiazoline-6-sulfonic acid) diammonium salt. <sup>d</sup> ZIF indicates zeolitic imidazolate framework nanosheets. <sup>e</sup> DAB indicates 3,3'-diaminobenzidine. <sup>f</sup> PBS indicates phosphate-buffered saline.

samples. The stability of nanozymes under different environmental conditions may affect the reliability of the detection results, which is a challenge in practical applications.<sup>257</sup>

### 7.6 Future prospects

To address the challenges of metal and metal oxide nanoparticle-assisted molecular detection methods in *E. coli* detection, future research directions may include the following. (i) Optimization of synthesis methods. The synthesis of nanomaterials may be improved through the use of green synthesis techniques and the optimization of synthesis conditions, with the aim of enhancing the biocompatibility and functionality of nanoparticles. (ii) Enhance material stability: optimize the synthesis pathways and surface modifications of nanomaterials to enhance their stability and reuse times, thereby ensuring that they maintain high performance after multiple uses. (iii) Enhance the specificity of the detection system: develop new types of specific bioprobes and explore the strategy of using multiple probes in combination to improve the specificity and sensitivity of detection. (iv) Simplification of sample pretreatment steps, which is another avenue for future research. The development of integrated detection platforms that integrate sample pretreatment and detection steps on a single platform is a promising approach that can reduce operational complexity and shorten detection times. (v) Development of multifunctional nanomaterials: the objective is to create nanomaterials with multiple functions, not only for detection purposes but also for treatment and prevention. (vi) Intelligent detection platform: the integration of artificial intelligence and the Internet of Things (IoT) technologies will facilitate the development of an intelligent detection platform that enables remote monitoring and real-time data analysis, thereby enhancing the efficiency and accuracy of detection. (vii) Mass production and standardization: it is recommended that nanomaterials be produced on a large scale, such that unified quality control and testing standards be established, that costs be reduced, and that penetration be increased. (viii) Development of novel nanozymes: a comprehensive investigation of the catalytic mechanism of nanozymes is essential for the development of more nanozymes with high substrate specificity and stability.

In conclusion, the use of metal and metal oxide nanoparticles in molecular detection methods has the potential to facilitate rapid, sensitive, and cost-effective detection of *E. coli*. It is anticipated that the utilization of metal and metal oxide nanoparticles in the detection of *E. coli* will become more sophisticated and effective, thereby facilitating greater contributions to the protection of public health and food safety.

## 8 Conclusion

This review comprehensively describes the wide range of applications of metal and metal oxide nanoparticles in *E. coli* detection, encompassing the entire molecular diagnostic process from sample pre-treatment to final detection. The article highlights the important applications of magnetic nanoparticles in

bacterial enrichment and nucleic acid purification as well as the remarkable effect of nanoparticle-assisted immunoassays and nucleic acid tests in enhancing detection efficiency and accuracy. In addition, the exploration of novel detection technologies, such as biosensors and artificial intelligence strategies, highlights the potential of nanoparticles in facilitating rapid and accurate detection of *E. coli*. These studies provide new strategies and tools for molecular diagnostics in food safety and public health, which are expected to play a key role in future practices.

## Author contributions

LLZ: conceptualization, methodology, formal analysis, writing – original draft, and writing – review & editing. JSG: conceptualization, methodology, formal analysis and writing – review & editing. DZ: conceptualization and formal analysis. PZ: methodology and formal analysis. YZ: methodology and formal analysis. LS: conceptualization. JBY: formal analysis and resources. YZ: conceptualization, methodology, formal analysis, and writing – review & editing. QPS: conceptualization, methodology, formal analysis, and writing – review & editing.

## Conflicts of interest

There are no conflicts to declare.

## Acknowledgements

We would like to express our gratitude to the researchers who conducted the studies and applied metal and metal oxide nanoparticle-assisted molecular assays for the detection of *E. coli*, as well as to all those who provided the references used in this review. We also acknowledge the support of the Natural Science Fund Project of Jiangsu Vocational College of Agriculture and Forestry (No. 2022kj32, 2023kj08), the Natural Science Fund Project of Colleges in Jiangsu Province (No. 22KJB180001), and the Teaching Innovation Team of Animal Husbandry and Veterinary in Jiangsu Province for this work.

## References

- 1 M. Mueller and C. R. Tainter, in *StatPearls*, StatPearls Publishing, Treasure Island (FL), 2024.
- 2 F. Carvalho, J. George, H. M. A. Sheikh and R. Selvin, *J. Biomed. Nanotechnol.*, 2018, **14**, 829–846.
- 3 A. Ben Aissa, J. J. Jara, R. M. Sebastián, A. Vallribera, S. Campoy and M. I. Pividori, *Biosens. Bioelectron.*, 2017, **88**, 265–272.
- 4 Z. Oushyani Roudsari, Y. Karami, S. S. Khoramrooz, S. Rouhi, H. Ghasem, S. H. Khatami, M. Alizadeh, N. Ahmad Khosravi, A. Mansoriyan, E. Ghasemi,

- A. Movahedpour and Z. Dargahi, *Clin. Chim. Acta*, 2024, **565**, 119984.
- 5 H. Lee, H. Han and S. Jeon, *Anal. Chem.*, 2021, **93**, 12237–12242.
- 6 Z. Li, J. Ma, J. Ruan and X. Zhuang, *Nanoscale Res. Lett.*, 2019, **14**, 195.
- 7 D. Wang, F. Lian, S. Yao, Y. Liu, J. Wang, X. Song, L. Ge, Y. Wang, Y. Zhao, J. Zhang, C. Zhao and K. Xu, *ACS Omega*, 2020, **5**, 23070–23080.
- 8 H. Ilhan, B. Guven, U. Dogan, H. Torul, S. Evran, D. Çetin, Z. Suludere, N. Saglam, İ. H. Boyaci and U. Tamer, *Talanta*, 2019, **201**, 245–252.
- 9 Z. Zhou, R. Xiao, S. Cheng, S. Wang, L. Shi, C. Wang, K. Qi and S. Wang, *Anal. Chim. Acta*, 2021, **1160**, 338421.
- 10 A. Jóskowiak, C. L. Nogueira, S. P. Costa, A. P. Cunha, P. P. Freitas and C. M. Carvalho, *Mikrochim. Acta*, 2023, **190**, 356.
- 11 J. Chen, S. D. Alcaine, Z. Jiang, V. M. Rotello and S. R. Nugen, *Anal. Chem.*, 2015, **87**, 8977–8984.
- 12 F. Pan, S. Altenried, S. Scheibler and Q. Ren, *Nanoscale*, 2024, **16**, 3011–3023.
- 13 Ü. Dogan, F. Sucularlı, E. Yildirim, D. Cetin, Z. Suludere, I. H. Boyaci and U. Tamer, *Biosensors*, 2022, **12**, 765.
- 14 J. Chen, B. Duncan, Z. Wang, L.-S. Wang, V. M. Rotello and S. R. Nugen, *Nanoscale*, 2015, **7**, 16230–16236.
- 15 C. M. Carmody and S. R. Nugen, *Sci. Rep.*, 2023, **13**, 16207.
- 16 F. Mi, M. Guan, Y. Wang, G. Chen, P. Geng and C. Hu, *Mikrochim. Acta*, 2023, **190**, 103.
- 17 Z. Ling, Q. Xu, Y. Song, W. Zhang and H. Xu, *Talanta*, 2024, **276**, 126273.
- 18 C. Boodoo, E. Dester, S. Asadullah Sharief and E. C. Alocilja, *J. Food Prot.*, 2023, **86**, 100066.
- 19 F. Mi, M. Guan, Y. Wang, G. Chen, P. Geng, Q. Cui and H. Huan, *Spectrochim. Acta, Part A*, 2023, **302**, 123094.
- 20 Y. Sun, C. Zhao, Z. Yan, J. Ren and X. Qu, *Chem. Commun.*, 2016, **52**, 7505–7508.
- 21 K. El-Boubbou, C. Gruden and X. Huang, *J. Am. Chem. Soc.*, 2007, **129**, 13392–13393.
- 22 X. He, L. Zhou, D. He, K. Wang and J. Cao, *Analyst*, 2011, **136**, 4183–4191.
- 23 N. Hasan, Z. Guo and H.-F. Wu, *Anal. Bioanal. Chem.*, 2016, **408**, 6269–6281.
- 24 Y. Xu, H. Wang, C. Luan, Y. Liu, B. Chen and Y. Zhao, *Biosens. Bioelectron.*, 2018, **100**, 404–410.
- 25 V. Kale, C. Chavan, S. Bhapkar, K. G. Girija and S. N. Kale, *Biomed. Phys. Eng. Express*, 2022, **8**(6), 065002.
- 26 K. Xu, J. Zhu, T. Zhang and G. Sui, *Talanta*, 2024, **278**, 126435.
- 27 Y. Che, Y. Xu, R. Wang and L. Chen, *Anal. Bioanal. Chem.*, 2017, **409**, 4709–4718.
- 28 H. Qi, Z. Zhong, H. Zhou, C. Deng, H. Zhu, J. Li, X. Wang and F. Li, *Int. J. Nanomed.*, 2011, **6**, 3033–3039.
- 29 S. Li, Z. Guo, Y. Liu, Z. Yang and H. K. Hui, *Talanta*, 2009, **80**, 313–320.
- 30 K. Yuan, Q. Mei, X. Guo, Y. Xu, D. Yang, B. J. Sánchez, B. Sheng, C. Liu, Z. Hu, G. Yu, H. Ma, H. Gao, C. Haisch, R. Niessner, Z. Jiang, Z. Jiang and H. Zhou, *Chem. Sci.*, 2018, **9**, 8781–8795.
- 31 M. L. Bhaisare, H. N. Abdelhamid, B.-S. Wu and H.-F. Wu, *J. Mater. Chem. B*, 2014, **2**, 4671–4683.
- 32 W. Lee, D. Kwon, W. Choi, G. Y. Jung and S. Jeon, *Sci. Rep.*, 2015, **5**, 7717.
- 33 S.-M. You, K. Luo, J.-Y. Jung, K.-B. Jeong, E.-S. Lee, M.-H. Oh and Y.-R. Kim, *ACS Appl. Mater. Interfaces*, 2020, **12**, 18292–18300.
- 34 Y. Xiao, S. Luo, J. Qiu, Y. Zhang, W. Liu, Y. Zhao, Y. Zhu, Y. Deng, M. Lu, S. Liu, Y. Lin, A. Huang, W. Wang, X. Hu and B. Gu, *J. Nanobiotechnol.*, 2024, **22**, 75.
- 35 J. Chen, X. Liu, Z. Liu, J. Ma, J. Han, Y. Sun, J. Liang, H. Han, J. Zhao, B. Wang, R. Xiao and Y. Wang, *Sens. Actuators, B*, 2024, **409**, 135598.
- 36 U. Tamer, D. Cetin, Z. Suludere, I. H. Boyaci, H. T. Temiz, H. Yegenoglu, P. Daniel, I. Dinçer and Y. Elerman, *Int. J. Mol. Sci.*, 2013, **14**, 6223–6240.
- 37 C. Zhang, C. Wang, R. Xiao, L. Tang, J. Huang, D. Wu, S. Liu, Y. Wang, D. Zhang, S. Wang and X. Chen, *J. Mater. Chem. B*, 2018, **6**, 3751–3761.
- 38 H. Kearns, R. Goodacre, L. E. Jamieson, D. Graham and K. Faulds, *Anal. Chem.*, 2017, **89**, 12666–12673.
- 39 J.-C. Liu, P.-J. Tsai, Y. C. Lee and Y.-C. Chen, *Anal. Chem.*, 2008, **80**, 5425–5432.
- 40 R. A. Bohara, N. D. Throat, N. A. Mulla and S. H. Pawar, *Appl. Biochem. Biotechnol.*, 2017, **182**, 598–608.
- 41 C.-T. Chen, J.-W. Yu and Y.-P. Ho, *J. Food Drug Anal.*, 2019, **27**, 575–584.
- 42 D. Kwon, S. Lee, M. M. Ahn, I. S. Kang, K.-H. Park and S. Jeon, *Anal. Chim. Acta*, 2015, **883**, 61–66.
- 43 S. Quintana-Sánchez, A. Barrios-Gumiel, J. Sánchez-Nieves, J. L. Copa-Patiño, F. J. de la Mata and R. Gómez, *Biomater. Adv.*, 2022, **133**, 112622.
- 44 C.-L. Chiang, C.-S. Sung, T.-F. Wu, C.-Y. Chen and C.-Y. Hsu, *J. Chromatogr. B: Anal. Technol. Biomed. Life Sci.*, 2005, **822**, 54–60.
- 45 Y. Shi, Y. Che, Y. Zhao, R. Ran, Y. Zhao, S. Yu, M. Chen, L. Dong, Z. Zhao and X. Wang, *J. Chromatogr. A*, 2024, **1724**, 464923.
- 46 E. Carloni, L. Rotundo, G. Brandi and G. Amagliani, *Folia Microbiol.*, 2018, **63**, 735–742.
- 47 F. Chen, S. Kim, J.-H. Na, K. Han and T. Y. Lee, *Mikrochim. Acta*, 2020, **187**, 558.
- 48 F. Firoozeh, A. Neshan, A. Khaledi, M. Zibaei, A. Amiri, A. Sobhani, F. Badmasti and V. S. Nikbin, *Polym. Bull.*, 2023, **80**, 3153–3163.
- 49 Z. Shan, C. Li, X. Zhang, K. D. Oakes, M. R. Servos, Q. Wu, H. Chen, X. Wang, Q. Huang, Y. Zhou and W. Yang, *Anal. Biochem.*, 2011, **412**, 117–119.
- 50 H.-P. Zhang, S. Bai, L. Xu and Y. Sun, *J. Chromatogr. B: Anal. Technol. Biomed. Life Sci.*, 2009, **877**, 127–133.
- 51 K. Jangpatarapongsa, K. Saimuang, D. Polpanich, R. Thiramanas, M. Techakasikornpanich, P. Yudech,

- V. Paripurana, C. Leepiyasakulchai and P. Tangboriboonrat, *Biotechnol. Rep.*, 2021, **32**, e00677.
- 52 X. Xu, J. Chen, B. Li, L. Tang and J. Jiang, *Analyst*, 2019, **144**, 1725–1730.
- 53 A. T. Abafogi, J. Kim, J. Lee, M. O. Mohammed, D. van Noort and S. Park, *Sensors*, 2020, **20**, 1202.
- 54 Y. Zhang, J. Su, T. Fu, W. Zhang, Y. Xiao and Y. Huang, *Analyst*, 2023, **148**, 4279–4282.
- 55 C. Wang, K. Xing, G. Zhang, M. Yuan, S. Xu, D. Liu, W. Chen, J. Peng, S. Hu and W. Lai, *Food Chem.*, 2019, **281**, 91–96.
- 56 Q. Guo, J. Han, S. Shan, D. Liu, S. Wu, Y. Xiong and W. Lai, *Biosens. Bioelectron.*, 2016, **86**, 990–995.
- 57 I. P. Alves and N. M. Reis, *Biosens. Bioelectron.*, 2019, **145**, 111624.
- 58 Y. Wang, T. Bu, Y. Cao, H. Wu, J. Xi, Q. Feng, C. Xuan and L. Wang, *Anal. Chem.*, 2023, **95**, 9237–9243.
- 59 N. Panchal, V. Jain, R. Elliott, Z. Flint, P. Worsley, C. Duran, T. Banerjee and S. Santra, *Anal. Chem.*, 2022, **94**, 13968–13977.
- 60 Y. Shao, W. Xu, Y. Zheng, J. Wang, J. Xie, Z. Zhu, X. Xiang, Q. Ye, Y. Zhang, L. Xue, B. Gu, J. Chen, J. Zhang, Q. Wu and Y. Ding, *Biosens. Bioelectron.*, 2022, **206**, 114150.
- 61 Y. Li, X. Chen, J. Yuan, Y. Leng, W. Lai, X. Huang and Y. Xiong, *J. Dairy Sci.*, 2020, **103**, 6940–6949.
- 62 W. Ren, D. R. Ballou, R. FitzGerald and J. Irudayaraj, *Biosens. Bioelectron.*, 2019, **126**, 324–331.
- 63 P. Wu, F. Xue, W. Zuo, J. Yang, X. Liu, H. Jiang, J. Dai and Y. Ju, *Anal. Chem.*, 2022, **94**, 4277–4285.
- 64 Y. Shao, Z. Wang, J. Xie, Z. Zhu, Y. Feng, S. Yu, L. Xue, S. Wu, Q. Gu, J. Zhang, Q. Wu, J. Wang and Y. Ding, *Food Chem.*, 2023, **424**, 136366.
- 65 G. Zhang, H. Hu, S. Deng, X. Xiao, Y. Xiong, J. Peng and W. Lai, *Biosens. Bioelectron.*, 2023, **225**, 115090.
- 66 Y. Tao, J. Yang, L. Chen, Y. Huang, B. Qiu, L. Guo and Z. Lin, *Mikrochim. Acta*, 2018, **185**, 350.
- 67 W. Shen, C. Wang, S. Zheng, B. Jiang, J. Li, Y. Pang, C. Wang, R. Hao and R. Xiao, *J. Hazard. Mater.*, 2022, **437**, 129347.
- 68 T. Bu, P. Jia, J. Liu, Y. Liu, X. Sun, M. Zhang, Y. Tian, D. Zhang, J. Wang and L. Wang, *Food Chem.: X*, 2019, **3**, 100052.
- 69 G. A. R. Y. Suaifan, S. Alhogail and M. Zourob, *Biosens. Bioelectron.*, 2017, **92**, 702–708.
- 70 H. Huang, G. Zhao and W. Dou, *Biosens. Bioelectron.*, 2018, **107**, 266–271.
- 71 H. Lee, J. Hwang, Y. Park, D. Kwon, S. Lee, I. Kang and S. Jeon, *RSC Adv.*, 2018, **8**, 26266–26270.
- 72 Z. Qiao, Q. Cai, Y. Fu, C. Lei and W. Yang, *Anal. Bioanal. Chem.*, 2021, **413**, 4417–4426.
- 73 A. H. A. Hassan, J. F. Bergua, E. Morales-Narváez and A. Mekoçi, *Food Chem.*, 2019, **297**, 124965.
- 74 T. Jiang, Y. Song, T. Wei, H. Li, D. Du, M. Zhu and Y. Lin, *Biosens. Bioelectron.*, 2016, **77**, 687–694.
- 75 L. Dou, Y. Bai, M. Liu, S. Shao, H. Yang, X. Yu, K. Wen, Z. Wang, J. Shen and W. Yu, *Biosens. Bioelectron.*, 2022, **204**, 114093.
- 76 X. Lai, G. Zhang, L. Zeng, X. Xiao, J. Peng, P. Guo, W. Zhang and W. Lai, *ACS Appl. Mater. Interfaces*, 2021, **13**, 1413–1423.
- 77 Z. Wang, X. Yao, Y. Zhang, R. Wang, Y. Ji, J. Sun, D. Zhang and J. Wang, *Food Chem.*, 2020, **329**, 127224.
- 78 Y. Yao, L. Hou, F. Wei, T. Lin and S. Zhao, *Analyst*, 2024, **149**, 357–365.
- 79 S. Bazsefidpar, E. Serrano-Pertierra, G. Gutiérrez, A. S. Calvo, M. Matos and M. C. Blanco-López, *Mikrochim. Acta*, 2023, **190**, 264.
- 80 K. He, T. Bu, X. Zheng, J. Xia, F. Bai, S. Zhao, X. Y. Sun, M. Dong and L. Wang, *J. Hazard. Mater.*, 2022, **425**, 128034.
- 81 Y. Wang, Q. Feng, H. Yan, R. Sun, Y. Cao, H. Wu, J. Xi, C. Xuan, J. Xia, B. Sun and L. Wang, *Anal. Chem.*, 2024, **96**, 1232–1240.
- 82 K. Xing, J. Peng, D. Liu, L. Hu, C. Wang, G. Li, G. Zhang, Z. Huang, S. Cheng, F. Zhu, N. Liu and W. Lai, *Anal. Chim. Acta*, 2018, **998**, 52–59.
- 83 H. Liu, C. Chen, C. Zhang, X. Du, P. Li and S. Wang, *J. Food Sci.*, 2019, **84**, 2916–2924.
- 84 C. Gondhalekar, E. Biela, B. Rajwa, E. Bae, V. Patsekin, J. Sturgis, C. Reynolds, I.-J. Doh, P. Diwakar, L. Stanker, V. Zorba, X. Mao, R. Russo and J. P. Robinson, *Anal. Bioanal. Chem.*, 2020, **412**, 1291–1301.
- 85 J. Han, L. Zhang, L. Hu, K. Xing, X. Lu, Y. Huang, J. Zhang, W. Lai and T. Chen, *J. Dairy Sci.*, 2018, **101**, 5770–5779.
- 86 P. Amornwairat and D. Pissuwan, *ACS Omega*, 2023, **8**, 13456–13464.
- 87 V. Soheili, S. M. Taghdisi, K. Abnous and M. Ebrahimi, *Iran. J. Basic Med. Sci.*, 2020, **23**, 901–908.
- 88 S. Ledlod, S. Areekit, S. Santiwatanakul and K. Chansiri, *Food Sci. Technol. Int.*, 2020, **26**, 430–443.
- 89 L. Zheng, G. Cai, S. Wang, M. Liao, Y. Li and J. Lin, *Biosens. Bioelectron.*, 2019, **124–125**, 143–149.
- 90 H. Peng and I. A. Chen, *ACS Nano*, 2019, **13**, 1244–1252.
- 91 J. Wang, Y. Cao, Z. Li, M. Dong, W. Dou, X. Xu and S. He, *Anal. Methods*, 2023, **15**, 275–283.
- 92 S. Wei, Q. Tang, X. Hu, W. Ouyang, H. Shao, J. Li, H. Yan, Y. Chen and L. Liu, *ACS Sens.*, 2024, **9**, 325–336.
- 93 K. Khachornsakkul, R. Del-Rio-Ruiz, H. Creasey, G. Widmer and S. R. Sonkusale, *ACS Sens.*, 2023, **8**, 4364–4373.
- 94 H. Shirzad, M. Panji, S. A. M. Nezhad, P. Houshmand and I. A. Tamai, *J. Microbiol. Methods*, 2024, **217–218**, 106858.
- 95 T. Yang, Z. Wang, Y. Song, X. Yang, S. Chen, S. Fu, X. Qin, W. Zhang, C. Man and Y. Jiang, *J. Dairy Sci.*, 2021, **104**, 8506–8516.
- 96 C. Wang, R. Deng, H. Li, Z. Liu, X. Niu and X. Li, *Mikrochim. Acta*, 2024, **191**, 454.
- 97 L. Gao, H. Wei, S. Dong and X. Yan, *Adv. Mater.*, 2024, **36**, 2305249.

- 98 X. Yuan, H. Cao, H. Zhang, G. Mao and L. Wei, *Spectrochim. Acta, Part A*, 2023, **299**, 122888.
- 99 Y. Wang, X. Cheng, C. Wang, D. Zhang, A. Liu, Z. Wang, W. Wei and S. Liu, *Talanta*, 2023, **264**, 124779.
- 100 S. Wang, D. Xu, C. Ding, Y. Tian, K. Ge, L. Guo, J. Li, Q. Dong, Y. Huang and Q. Liu, *Mikrochim. Acta*, 2020, **187**, 506.
- 101 S. Mumtaz, L.-S. Wang, S. Z. Hussain, M. Abdullah, Z. Huma, Z. Iqbal, B. Creran, V. M. Rotello and I. Hussain, *Chem. Commun.*, 2017, **53**, 12306–12308.
- 102 M. Liu, F. Zhang, S. Dou, J. Sun, F. Vriesekoop, F. Li, Y. Guo and X. Sun, *Anal. Methods*, 2023, **15**, 1661–1667.
- 103 T. N. Le, T. D. Tran and M. I. Kim, *Nanomaterials*, 2020, **10**, 92.
- 104 D. Zhang, X. Zhang, X. Li, N. Wang and X. Zhao, *Talanta*, 2024, **280**, 126783.
- 105 T. Lin, Y. Lai, G. Jiang, X. Chen, L. Hou and S. Zhao, *Chem. Commun.*, 2023, **59**, 12986–12989.
- 106 Y. Guo, J. Zhao, X. Ma, M. Cai, S. Liu, C. Sun, Y. Chi and K. Xu, *Microbiol. Spectrum*, 2024, **12**, e0397823.
- 107 S. U. Kim, E.-J. Jo, H. Mun, Y. Noh and M.-G. Kim, *J. Agric. Food Chem.*, 2018, **66**, 4941–4947.
- 108 S. K. Gahlaut, N. Kalyani, C. Sharan, P. Mishra and J. P. Singh, *Biosens. Bioelectron.*, 2019, **126**, 478–484.
- 109 X. Liu, W. Li, J. Sun, S. Dai, X. Wang, J. Yang, Q. Li, Y. Li, H. Ge, J. Zhao and J. Li, *Food Chem.*, 2023, **423**, 136339.
- 110 N. Al-Awwal, M. Masjedi, M. El-Dweik, S. H. Anderson and J. Ansari, *J. Microbiol. Methods*, 2022, **193**, 106403.
- 111 C. Cheng, L. Yang, M. Zhong, W. Deng, Y. Tan, Q. Xie and S. Yao, *Analyst*, 2018, **143**, 4067–4073.
- 112 F. Lian, D. Wang, S. Yao, L. Ge, Y. Wang, Y. Zhao, J. Zhao, X. Song, C. Zhao, J. Li, Y. Liu, M. Jin and K. Xu, *Food Sci. Biotechnol.*, 2021, **30**, 1129–1138.
- 113 N. Amin, A. S. Torralba, R. Álvarez-Diduk, A. Afkhami and A. Merkoçi, *Anal. Chem.*, 2020, **92**, 4209–4216.
- 114 A. Pant, T. Kaur, T. Sharma, J. Singh, A. Suttee, R. P. Barnwal, I. P. Kaur, G. Singh and B. Singh, *J. Water Health*, 2022, **20**, 1673–1687.
- 115 Ü. Dogan, E. N. Kasap, F. Sicularlı, E. Yildirim, U. Tamer, D. Cetin, Z. Suludere, I. H. Boyaci and N. Ertas, *Anal. Methods*, 2020, **12**, 3788–3796.
- 116 E. N. Kasap, Ü. Doğan, F. Çoğun, E. Yıldırım, İ. H. Boyacı, D. Çetin, Z. Suludere, U. Tamer and N. Ertaş, *J. Microbiol. Methods*, 2019, **164**, 105680.
- 117 P. Wu, R. Huang, G. Li, Y. He, C. Chen, W. Xiao and P. Ding, *J. Nanosci. Nanotechnol.*, 2018, **18**, 3654–3659.
- 118 S. G. Roh, A. I. Robby, P. T. M. Phuong, I. In and S. Y. Park, *Mater. Sci. Eng., C*, 2019, **97**, 613–623.
- 119 B. Heli and A. Ajji, *Sci. Rep.*, 2020, **10**, 14367.
- 120 C. Hunsur Ravikumar, S. R and R. G. Balakrishna, *J. Photochem. Photobiol., B*, 2020, **204**, 111799.
- 121 B. Fang, X. Liu, J. Peng, Y. Li, Z. Gong and W. Lai, *Food Chem.*, 2024, **445**, 138749.
- 122 S. Ghayyem and F. Faridbod, *Anal. Methods*, 2022, **14**, 813–819.
- 123 L. Xue, F. Huang, L. Hao, G. Cai, L. Zheng, Y. Li and J. Lin, *Food Chem.*, 2020, **322**, 126719.
- 124 N. R. Nirala and G. Shtenberg, *Spectrochim. Acta, Part A*, 2021, **257**, 119769.
- 125 F. Huang, H. Zhang, L. Wang, W. Lai and J. Lin, *Biosens. Bioelectron.*, 2018, **100**, 583–590.
- 126 H. Xu, F. Tang, J. Dai, C. Wang and X. Zhou, *BMC Microbiol.*, 2018, **18**, 100.
- 127 L. Ye, G. Zhao and W. Dou, *Talanta*, 2018, **182**, 354–362.
- 128 S. Bu, K. Wang, C. Wang, Z. Li, Z. Hao, W. Liu and J. Wan, *Mikrochim. Acta*, 2020, **187**, 679.
- 129 T. Shelby, S. Sulthana, J. McAfee, T. Banerjee and S. Santra, *J. Visualized Exp.*, 2017, 55821.
- 130 K. Wang, S. Bu, C. Ju, Y. Han, C. Ma, W. Liu, Z. Li, C. Li and J. Wan, *Mikrochim. Acta*, 2019, **186**, 57.
- 131 L. Su, B. Liu, Y. Cui and Y. Su, *Mikrochim. Acta*, 2023, **190**, 51.
- 132 L. Zheng, W. Dong, C. Zheng, Y. Shen, R. Zhou, Z. Wei, Z. Chen and Y. Lou, *Colloids Surf., B*, 2022, **212**, 112349.
- 133 Y. Li, Y. Xu, W. C. Soko and H. Bi, *Talanta*, 2024, **273**, 125880.
- 134 X. Li, S. Dong, P. Arul, H. Liu, L. Liu, H. Wang, Q. Zhang, E. Gyimah, S. Yakubu and Z. Zhang, *Talanta*, 2020, **214**, 120859.
- 135 G. Tatulli and P. P. Pompa, *Nanoscale*, 2020, **12**, 15604–15610.
- 136 E. Dester, K. Kao and E. C. Alocilja, *Biosensors*, 2022, **12**, 274.
- 137 Z. Wang, Q. Lu, T. Xu, F. Wang, F. Huang, Y. Peng and L. Deng, *Mikrochim. Acta*, 2020, **187**, 308.
- 138 H. Yang, M. Xiao, W. Lai, Y. Wan, L. Li and H. Pei, *Anal. Chem.*, 2020, **92**, 4990–4995.
- 139 X. Hu, Y. Li, Y. Xu, Z. Gan, X. Zou, J. Shi, X. Huang, Z. Li and Y. Li, *Food Chem.*, 2021, **339**, 127775.
- 140 X. Bai, L. Ga and J. Ai, *Analyst*, 2023, **148**, 3892–3898.
- 141 D. Li, E. Yang, Z. Luo, Q. Xie and Y. Duan, *Nanoscale*, 2021, **13**, 2492–2501.
- 142 C. Wang, Y. Zhang, W. Gong and S. Wang, *Luminescence*, 2024, **39**, e4716.
- 143 Q. Zhang, Y. Liu, Y. Nie, Q. Ma and B. Zhao, *Mikrochim. Acta*, 2019, **186**, 656.
- 144 A. J. Sami, S. Bilal, N.-U.-A. Ahsan, N. Hameed and S. Saleem, *Environ. Monit. Assess.*, 2023, **195**, 1442.
- 145 S. M. Saad, J. Abdullah, S. A. Rashid, Y. W. Fen, F. Salam and L. H. Yih, *Mikrochim. Acta*, 2019, **186**, 804.
- 146 H. Yan, L. Wu, J. Wang, Y. Zheng, F. Zhao, Q. Bai, H. Hu, H. Liang and X. Niu, *Anal. Methods*, 2024, **16**, 496–502.
- 147 M. Liu, L. Geng, F. Zhang, S. Dou, F. Li, Z. Liu, Y. Guo and X. Sun, *J. Agric. Food Chem.*, 2022, **70**, 15990–15998.
- 148 M. Schwarz, S. Pahlow, T. Bocklitz, C. Steinbrücker, D. Cialla, K. Weber and J. Popp, *Analyst*, 2013, **138**, 5866–5870.
- 149 S. S. Arumugam, A. W. Varghese, S. Suresh Nair and N. Y. Lee, *Anal. Methods*, 2023, **15**, 5793–5802.
- 150 I. A. Quintela, B. G. de los Reyes, C.-S. Lin and V. C. H. Wu, *Nanoscale*, 2015, **7**, 2417–2426.

- 151 X. Wang, S. Ying, X. Wei and J. Yuan, *Int. J. Food Microbiol.*, 2017, **253**, 66–74.
- 152 P. Teawprasong, Y. Wongngam, T. Tangchaikeeree, A. Elaissari, P. Tangboriboonrat, D. Polpanich and K. Jangpatarapongsa, *Sci. Rep.*, 2022, **12**, 20677.
- 153 Y. Song, M. Chen, L. Han, Z. Yan, L. Pan and K. Tu, *Anal. Chim. Acta*, 2023, **1239**, 340751.
- 154 S. Doughan, U. Uddayasankar, A. Peri and U. J. Krull, *Anal. Chim. Acta*, 2017, **962**, 88–96.
- 155 Y. Zeng, P. Qi, Y. Zhou, Y. Wang, Y. Xin, Y. Sun and D. Zhang, *Mikrochim. Acta*, 2022, **189**, 403.
- 156 J. Li, X. Liang, J. Ma, J. Cheng, H. Wang, X. Wang, J. J. Wu and H. An, *Micromachines*, 2024, **15**, 435.
- 157 M. Wang, Z. Liu, C. Liu, W. He, D. Qin and M. You, *Biosens. Bioelectron.*, 2024, **251**, 116122.
- 158 X. Liu, S. Bu, H. Wei, Z. Wang, S. Yu, Z. Li, Z. Hao, X. He and J. Wan, *Anal. Methods*, 2021, **13**, 3379–3385.
- 159 Y. Ren, P. Gao, Y. Song, X. Yang, T. Yang, S. Chen, S. Fu, X. Qin, M. Shao, C. Man and Y. Jiang, *J. Dairy Sci.*, 2021, **104**, 8517–8529.
- 160 J. R. Choi, J. Hu, R. Tang, Y. Gong, S. Feng, H. Ren, T. Wen, X. Li, W. A. Wan Abas, B. Pinguang-Murphy and F. Xu, *Lab Chip*, 2016, **16**, 611–621.
- 161 J. M. Kim, J. S. Park, T. H. Yoon, J. Park and K. S. Park, *Anal. Bioanal. Chem.*, 2021, **413**, 5003–5011.
- 162 B. Jin, B. Ma, Q. Mei, S. Xu, X. Deng, Y. Hong, J. Li, H. Xu and M. Zhang, *Biosensors*, 2023, **13**, 652.
- 163 S. Cui, Y. Wei, C. Li, J. Zhang, Y. Zhao, X. Peng and F. Sun, *Foods*, 2024, **13**, 2143.
- 164 H. Y. Kim, K. S. Park and H. G. Park, *Theranostics*, 2020, **10**, 4507–4514.
- 165 D. Liu, X. Yu, C. Li, Y. Wang, C. Huang, M. Li, Y. Huang and C. Yang, *ACS Appl. Mater. Interfaces*, 2024, **16**, 34632–34640.
- 166 D. Brandão, S. Liébana, S. Campoy, M. P. Cortés, S. Alegret and M. I. Pividori, *Biosens. Bioelectron.*, 2015, **74**, 652–659.
- 167 S. Viveiros, M. Rodrigues, D. Albuquerque, S. A. M. Martins, S. Cardoso and V. C. Martins, *Sensors*, 2020, **20**, 3351.
- 168 A. Rabti, R. Zayani, M. Meftah, I. Salhi and N. Raouafi, *Mikrochim. Acta*, 2020, **187**, 635.
- 169 C. O. Duya, F. O. Okumu and M. C. Matoetoe, *Bioelectrochemistry*, 2023, **151**, 108403.
- 170 S. Hargol Zadeh, S. Kashanian and M. Nazari, *Biosensors*, 2023, **13**, 619.
- 171 S. Nadzirah, U. Hashim, S. C. B. Gopinath, N. A. Parmin, A. A. Hamzah, H. W. Yu and C. F. Dee, *Mikrochim. Acta*, 2020, **187**, 235.
- 172 M. Sedki, X. Chen, C. Chen, X. Ge and A. Mulchandani, *Biosens. Bioelectron.*, 2020, **148**, 111794.
- 173 H. Kaur, M. Shorie and P. Sabherwal, *Mikrochim. Acta*, 2020, **187**, 461.
- 174 D. Wilson, E. M. Materón, G. Ibáñez-Redín, R. C. Faria, D. S. Correa and O. N. Oliveira, *Talanta*, 2019, **194**, 611–618.
- 175 D. Butler and A. Ebrahimi, *Methods Mol. Biol.*, 2022, **2393**, 447–471.
- 176 N. Abdelhamied, F. Abdelrahman, A. El-Shibiny and R. Y. A. Hassan, *Sci. Rep.*, 2023, **13**, 3498.
- 177 N. Shoaie, M. Forouzandeh and K. Omidfar, *Mikrochim. Acta*, 2018, **185**, 217.
- 178 D. Q. Nguyen, K. Ishiki and H. Shiigi, *Mikrochim. Acta*, 2018, **185**, 465.
- 179 D. Gunasekaran, Y. Gerchman and S. Vernick, *Biosensors*, 2022, **12**, 36.
- 180 M. Qaanei, R. A. Taheri and K. Eskandari, *Anal. Methods*, 2021, **13**, 3101–3109.
- 181 Y. Xu, Y. Dai, C. Li, H. Zhang, M. Guo and Y. Yang, *Rev. Sci. Instrum.*, 2020, **91**, 014103.
- 182 K. Al-Yahmadi, H. H. Kyaw, M. T. Z. Myint, R. Al-Mamari, S. Dobretsov and M. Al-Abri, *Discover Nano*, 2023, **18**, 45.
- 183 K. N. Fatema, Y. Liu, K. Y. Cho and W.-C. Oh, *ACS Omega*, 2020, **5**, 22719–22730.
- 184 S. Bazsefidpar, M. Freitas, C. R. Pereira, G. Gutiérrez, E. Serrano-Pertierra, H. P. A. Nouws, M. Matos, C. Delerue-Matos and M. C. Blanco-López, *Biosensors*, 2023, **13**, 567.
- 185 I. Salhi, A. Rabti, A. Dhehibi and N. Raouafi, *Int. J. Mol. Sci.*, 2022, **23**, 6028.
- 186 L. Yuwen, X. Li, L. Wu, Y. Luo and S. Su, *Analyst*, 2023, **148**, 6292–6296.
- 187 T. Das, S. Das and B. C. A, *ACS Biomater. Sci. Eng.*, 2024, **10**, 4018–4034.
- 188 A. G. Carota, A. Bonini, M. Urban, N. Poma, F. M. Vivaldi, A. Tavanti, M. Rossetti, G. Rosati, A. Merkoçi and F. Di Francesco, *Biosens. Bioelectron.*, 2024, **258**, 116340.
- 189 J. Zhang, W. Liu, J. Li, K. Lu, H. Wen and J. Ren, *Talanta*, 2022, **249**, 123646.
- 190 J. Yoo, H. Jeong, S. K. Park, S. Park and J. S. Lee, *Biosensors*, 2021, **11**, 212.
- 191 D. Jiang, C. Yang, Y. Fan, H.-M. Polly Leung, K. Inthavong, Y. Zhang, Z. Li and M. Yang, *Biosens. Bioelectron.*, 2021, **183**, 113214.
- 192 M. Wang, M. Wang, S. Huang, S. Zhang, Z. Zhang, L. He and M. Du, *Anal. Chim. Acta*, 2023, **1248**, 340893.
- 193 E. Huo, S. Shahab, H. Dang, Q. Jia and M. Wang, *Mikrochim. Acta*, 2023, **190**, 407.
- 194 L. Su, Y. Su and B. Liu, *Anal. Methods*, 2022, **14**, 2541–2548.
- 195 R. Gangwar, K. T. Rao, S. Khatun, A. K. Rengan, C. Subrahmanyam and S. R. Krishna Vanjari, *Anal. Chim. Acta*, 2022, **1233**, 340482.
- 196 S. Li, J. Liu, Z. Chen, Y. Lu, S. S. Low, L. Zhu, C. Cheng, Y. He, Q. Chen, B. Su and Q. Liu, *Sens. Actuators, B*, 2019, **297**, 126811.
- 197 F. Zhu, G. Zhao and W. Dou, *Anal. Biochem.*, 2018, **559**, 34–43.
- 198 M. Yin, C. Liu, R. Ge, Y. Fang, J. Wei, X. Chen, Q. Chen and X. Chen, *Biosens. Bioelectron.*, 2022, **203**, 114022.
- 199 L. Yang, X. Wang, X. Jing, B. Bai, T. Bo, J. Zhang, L. Yu, H. Qian, Y. Gu and Y. Yang, *Food Chem.*, 2024, **464**, 141591.

- 200 S. Khan, Akrema, S. Qazi, R. Ahmad, K. Raza and Rahisuddin, *ACS Omega*, 2021, **6**, 16076–16085.
- 201 S. Itagaki, A. Nakao, S. Nakamura, M. Fujita, S. Nishii, Y. Yamamoto, Y. Sadanaga and H. Shiigi, *Anal. Chem.*, 2024, **96**, 3787–3793.
- 202 C. Pandit, H. K. Alajangi, J. Singh, A. Khajuria, A. Sharma, M. S. Hassan, M. Parida, A. D. Semwal, N. Gopalan, R. K. Sharma, A. Suttee, U. Soni, B. Singh, S. Sapra, R. P. Barnwal, G. Singh and I. P. Kaur, *Sci. Total Environ.*, 2022, **831**, 154857.
- 203 B. Jin, S. Wang, M. Lin, Y. Jin, S. Zhang, X. Cui, Y. Gong, A. Li, F. Xu and T. J. Lu, *Biosens. Bioelectron.*, 2017, **90**, 525–533.
- 204 M. Yin, C. Wu, H. Li, Z. Jia, Q. Deng, S. Wang and Y. Zhang, *ACS Omega*, 2019, **4**, 8953–8959.
- 205 P. Halkare, N. Punjabi, J. Wangchuk, S. Madugula, K. Kondabagil and S. Mukherji, *ACS Sens.*, 2021, **6**, 2720–2727.
- 206 Z. Lian, C. Li, Y. Wang, L. Tan, M. Yu, L. Xiao, L. He, W. Gao, Y. Liu, Y. Ma, J. Hu, X. Luo and A. Li, *Anal. Chem.*, 2024, **96**, 18690–18698.
- 207 Y. Weng, X. Hu, L. Jiang, Q. Shi and X. Wei, *Anal. Bioanal. Chem.*, 2021, **413**, 5419–5426.
- 208 W. Zhao, S. Yang, D. Zhang, T. Zhou, J. Huang, M. Gao, Y. Jiang, Y. Liu and J. Yang, *J. Colloid Interface Sci.*, 2023, **634**, 651–663.
- 209 J. Chen, Y. Zeng, D. Zhang, P. Qi, X. Liu, R. Song and P. Wang, *Mikrochim. Acta*, 2023, **191**, 17.
- 210 Y. Ye, X. Qi, H. Wang, B. Zhao, L. Xu, Y. Zhang, X. Wang and N. Zhou, *Anal. Chim. Acta*, 2022, **1221**, 340141.
- 211 X. Wang, W. Li, S. Dai, M. Dou, S. Jiao, J. Yang, W. Li, Y. Su, Q. Li and J. Li, *Food Chem.*, 2023, **424**, 136433.
- 212 Y. Liu, W. Zhu, Q. Yuan, J. Hu, X. Zhang and A. Shen, *Talanta*, 2022, **245**, 123450.
- 213 A. Zhu, S. Ali, Z. Wang, Y. Xu, R. Lin, T. Jiao, Q. Ouyang and Q. Chen, *Anal. Chem.*, 2023, **95**, 18415–18425.
- 214 P. Wang, Y. Liu, X. Li, C. Li and G. Li, *Mikrochim. Acta*, 2024, **191**, 441.
- 215 Y. Liu, G. Su, W. Wang, H. Wei and L. Dang, *Anal. Methods*, 2024, **16**, 2085–2092.
- 216 A. Yadav, A. K. Yadav and N. Tarannum, *ACS Appl. Bio Mater.*, 2024, **7**, 6127–6137.
- 217 X. Qu, G. You and S. Wang, *Spectrochim. Acta, Part A*, 2024, **322**, 124850.
- 218 X. Zhu, Y. Ning, Z. Zhang, Y. Wen, Y. Zhao and H. Wang, *Anal. Bioanal. Chem.*, 2023, **415**, 1529–1543.
- 219 W. Shang, H. Xin, X. Hou, L. Wu and L. Wu, *ACS Appl. Mater. Interfaces*, 2024, **16**, 51679–51689.
- 220 L. Mahmudin, R. Wulandani, M. Riswan, E. Kurnia Sari, P. Dwi Jayanti, M. Syahrul Ulum, M. Arifin and E. Suharyadi, *Spectrochim. Acta, Part A*, 2024, **311**, 123985.
- 221 S. D. Gür, M. Bakhshpour and A. Denizli, *Mater. Sci. Eng., C*, 2019, **104**, 109869.
- 222 T. Banerjee, N. Panchal, C. Sutton, R. Elliott, T. Patel, K. Kajal, E. Arogunyo, N. Koti and S. Santra, *Biosensors*, 2023, **13**, 109.
- 223 C. Zhou, H. Zou, M. Li, C. Sun, D. Ren and Y. Li, *Biosens. Bioelectron.*, 2018, **117**, 347–353.
- 224 E. R. Wikantyasning, M. Da'i, Z. Choliso and U. Kalsum, *J. Pharm. BioAllied Sci.*, 2023, **15**, 81–87.
- 225 M. Basak, S. Mitra, M. Gogoi, S. Sinha, H. B. Nemade and D. Bandyopadhyay, *ACS Appl. Bio Mater.*, 2022, **5**, 5321–5332.
- 226 Y. Zhu, J. Wang, Y. Sun and Q. Cai, *Analyst*, 2020, **145**, 4436–4441.
- 227 F. Zheng, P. Wang, Q. Du, Y. Chen and N. Liu, *Front. Chem.*, 2019, **7**, 232.
- 228 C. Venkatachalaiah, U. Venkataraman and R. Sellappan, *IET Nanobiotechnol.*, 2020, **14**, 761–765.
- 229 Y. Shang, G. Xing, H. Lin, S. Chen, T. Xie and J. Lin, *Anal. Chem.*, 2023, **95**, 13368–13375.
- 230 F. Yang, L. Chen, H. Zhou, Q. Zhang, T. Hao, Y. Hu, S. Wang and Z. Guo, *Talanta*, 2024, **278**, 126550.
- 231 R. Meraat, K. Issazadeh, A. Abdolazadeh Ziabari and M. Faezi Ghasemi, *Curr. Microbiol.*, 2020, **77**, 2633–2641.
- 232 Z. Vaezi, M. Azizi, S. Sadeghi Mohammadi, N. Hashemi and H. Naderi-Manesh, *Talanta*, 2020, **218**, 121137.
- 233 X. Wang, W. Chen, H. Yang, X. Zhang, M. Deng, X. Zhou, K. Huang, P. Chen and B. Ying, *Mikrochim. Acta*, 2020, **187**, 453.
- 234 X. Liao, W. Tong, L. Dai, L. Han, H. Sun, W. Liu and C. Wang, *J. Mater. Chem. B*, 2023, **11**, 4890–4898.
- 235 F. Safir, N. Vu, L. F. Tadesse, K. Firouzi, N. Banaei, S. S. Jeffrey, A. A. E. Saleh, B. P. T. Khuri-Yakub and J. A. Dionne, *Nano Lett.*, 2023, **23**, 2065–2073.
- 236 G. Xie, S. Du, Q. Huang, M. Mo, Y. Gao, M. Li, J. Tao, L. Zhang and J. Zhu, *ACS Appl. Mater. Interfaces*, 2022, **14**, 5856–5866.
- 237 H. Mann, S. Khan, A. Prasad, F. Bayat, J. Gu, K. Jackson, Y. Li, Z. Hosseinidoust, T. F. Didar and C. D. M. Filipe, *Adv. Mater.*, 2025, **37**, e2411173.
- 238 A. I. Robby and S. Y. Park, *Anal. Chim. Acta*, 2019, **1082**, 152–164.
- 239 X. Li, X. Li, J. Chen, Z. Tan and C. Wang, *Anal. Biochem.*, 2024, **692**, 115559.
- 240 Y. Xiong, X. Zeng, L. Yan, Y. Wang, Y. Lin, K. Ao, P. Feng, Y. Xie and P. Chen, *ACS Appl. Mater. Interfaces*, 2023, **15**, 27687–27695.
- 241 X. Mou, X. Chen, J. Wang, Z. Zhang, Y. Yang, Z. Shou, Y. Tu, X. Du, C. Wu, Y. Zhao, L. Qiu, P. Jiang, C. Chen, D. Huang and Y. Li, *ACS Appl. Mater. Interfaces*, 2019, **11**, 23093–23101.
- 242 J. Hong, L. Wang, Q. Zheng, C. Cai, X. Yang and Z. Liao, *Materials*, 2024, **17**, 2870.
- 243 Y. Chen, Y. Liu, Y. Shi, J. Ping, J. Wu and H. Chen, *TrAC, Trends Anal. Chem.*, 2020, **127**, 115912.
- 244 Y. Chen, J. Lin, Q. Jiang, Q. Chen, S. Zhang and L. Li, *J. Nanosci. Nanotechnol.*, 2016, **16**, 2296–2300.
- 245 A. J. Franco and E. Alocilja, *Cells*, 2025, **14**, 225.
- 246 J. Kang, Y. Li, Y. Zhao, Y. Wang, C. Ma and C. Shi, *Anal. Biochem.*, 2021, **635**, 114445.

- 247 F. Bai, T. Bu, Z. Wang and B. Shao, *Nano Today*, 2024, **57**, 102403.
- 248 H. Gong, Q. Zeng, S. Gai, Y. Du, J. Zhang, Q. Wang, H. Ding, L. Wu, A. A. Ansari and P. Yang, *Chin. Chem. Lett.*, 2024, 110059.
- 249 C. Yi, Z. Luo, Y. Lu, T. Belwal, X. Pan and X. Lin, *Biosens. Bioelectron.*, 2021, **184**, 113199.
- 250 Y. Dong, S. Mao, S. Chen, J. Ma, N. Jaffrezic-Renault and Z. Guo, *TrAC, Trends Anal. Chem.*, 2024, **180**, 117891.
- 251 Z. Guo, H. Jiang, A. Song, X. Liu and X. Wang, *Adv. Colloid Interface Sci.*, 2024, **332**, 103265.
- 252 G. Xing, Y. Shang, J. Ai, H. Lin, Z. Wu, Q. Zhang, J. Lin, Q. Pu and L. Lin, *Anal. Chem.*, 2023, **95**, 13391–13399.
- 253 S. Bu, K. Wang, H. Bai, Y. Leng, C. Ju, C. Wang, W. Liu and J. Wan, *Mikrochim. Acta*, 2019, **186**, 296.
- 254 J. Li, J. Xue, Y. Zhang, Y. He and Z. Fu, *ACS Sens.*, 2022, **7**, 2438–2445.
- 255 C. Lu, L. Tang, F. Gao, Y. Li, J. Liu and J. Zheng, *Biosens. Bioelectron.*, 2021, **187**, 113327.
- 256 S. Mansouri, *Microchem. J.*, 2024, **205**, 111392.
- 257 Z. Su, T. Du, X. Liang, X. Wang, L. Zhao, J. Sun, J. Wang and W. Zhang, *Food Control*, 2022, **141**, 109165.